rec'd w/cover letter dtd 2/11/87

Final Version Sent to Diane(NS)/WMP 01/12/88

Version of February 11, 1987

GEOCHEMISTRY SIMULATION OF YUCCA MOUNTAIN: MODELING THE TRANSPORT OF URANIUM AND TECHNETIUM THROUGH THE UNSATURATED TUFFS

(NNWSI Milestone M325: Level I)

TWS-ESS-5/6-86-01

Gail A. Cederberg, L. Eric Greenwade, and Bryan J. Travis
Earth and Space Sciences Division

Los Alamos National Laboratory
Los Alamos, New Mexico 87545

TWS NO. V ORIGINATOR ~ TITLE/SUBJECT ~

WBS NO. 1.2.3.4.1.7.A QA LEVEL

DOC. TYPE WETI DOC. DATE 2/11/87

1028

9307090240 930617
PDR WASTE
WM-11 PDR

CONTENTS

LIST OF TABLES 3

LIST OF FIGURES 3

ABSTRACT 5

I. EXECUTIVE SUMMARY 6

II. INTRODUCTION 7

III. GEOCHEMICAL/GEOPHYSICAL MODEL 9
- A. Stratigraphy 9
- B. Properties of the Geologic Media 10
- C. Hydrogeology 11
- D. Geochemistry 12
- E. Source Term 13

IV. NUMERICAL SIMULATIONS 14
- A. TRACR3D 14
- B. Scenarios 16

V. RESULTS 16
- A. Uranium Transport 16
- B. Technetium Transport 17
- C. Effects of Sorption 20
- D. Effects of Flow 21

VI. DISCUSSION 21
- A. Geochemical/Geophysical Model 21
- B. Transport Calculations 22

VII. CONCLUSIONS AND RECOMMENDATIONS 23
- A. Conclusions 24
- B. Recommendations 24

REFERENCES 26

-20386 0211

LIST OF TABLES

Table I. Material Properties of the Stratigraphic Units

Table II. Available and Estimated Distribution Coefficients, K_d's, for Yucca Mountain Tuffs

Table III. Scenarios for the Numerical Simulations of Uranium and Technetium Transport

LIST OF FIGURES

Figure 1. Schematic representation of Yucca Mountain stratigraphy (not to scale).

Figure 2. Liquid-phase concentrations during transport of ^{238}U through unsaturated Yucca Mountain tuff at normal flow rate. Adjacent lines differ in concentration by a factor of 10. u_z = 0.5 mm/yr. t = 5,000, 10,000, and 15,000 yr. (Case 1)

Figure 3. Sorbed concentrations during transport of ^{238}U through unsaturated Yucca Mountain tuff at normal flow rate. Adjacent lines differ in concentration by a factor of 10. u_z = 0.5 mm/yr. t = 5,000, 10,000, and 15,000 yr. (Case 1)

Figure 4. Liquid-phase concentrations during transport of ^{238}U through unsaturated Yucca Mountain tuff at high flow rate. Adjacent lines differ in concentration by a factor of 10. u_z = 4.5 mm/yr. t = 5,000, 10,000, and 15,000 yr. (Case 2)

Figure 5. Sorbed concentrations during transport of ^{238}U through unsaturated Yucca Mountain tuff at high flow rate. Adjacent lines differ in concentration by a factor of 10. u_z = 4.5 mm/yr. t = 5,000, 10,000, and 15,000 yr. (Case 2)

Figure 6. Comparison of liquid-phase concentrations of ^{238}U after transport for 10,000 yr at different flow rates (Cases 1 and 2). Adjacent lines differ in concentration by a factor of 10.

Figure 7. Liquid-phase concentrations during transport of ^{99}Tc with sorption through unsaturated Yucca Mountain tuff at normal flow rate. Adjacent lines differ in concentration by a factor of 10. u_z = 0.5 mm/yr. t = 5,000, 10,000, and 15,000 yr. (Case 3)

Figure 8. Sorbed concentrations during transport of ^{99}Tc with sorption through unsaturated Yucca Mountain tuff at normal flow rate. Adjacent lines differ in concentration by a factor of 10. u_z = 0.5 mm/yr. t = 5,000, 10,000, and 15,000 yr. (Case 3)

Figure 9. Liquid-phase concentrations during transport of ^{99}Tc with sorption through unsaturated Yucca Mountain tuff at high flow rate. Adjacent lines differ in concentration by a factor of 10. u_z = 4.5 mm/yr. t = 5,000, 10,000, and 15,000 yr. (Case 4)

Figure 10. Sorbed concentrations during transport of ^{99}Tc with sorption through unsaturated Yucca Mountain tuff at high flow rate. Adjacent lines differ in concentration by a factor of 10. u_z = 4.5 mm/yr. t = 5,000, 10,000, and 15,000 yr. (Case 4)

Figure 11. Comparison of liquid-phase concentrations of ^{99}Tc after transport with sorption for 10,000 yr at different flow rates (Cases 3 and 4). Adjacent lines differ in concentration by a factor of 10.

Figure 12. Liquid-phase concentrations during transport of ^{99}Tc without sorption through unsaturated Yucca Mountain tuff at normal flow rate. Adjacent lines differ in concentration by a factor of 10. u_z = 0.5 mm/yr. t = 5,000, 10,000, and 15,000 yr. (Case 5)

Figure 13. Liquid-phase concentrations during transport of ^{99}Tc without sorption through unsaturated Yucca Mountain tuff at high flow rate. Adjacent lines differ in concentration by a factor of 10. u_z = 4.5 mm/yr. t = 5,000 and 10,000 yr. (Case 6)

Figure 14. Comparison of liquid-phase concentrations of ^{99}Tc after transport without sorption for 10,000 yr at different flow rates (Cases 5 and 6). Adjacent lines differ in concentration by a factor of 10.

Figure 15. Effect of sorption on liquid-phase concentration of ^{99}Tc after transport through Yucca Mountain tuff at normal flow rate for 10,000 yr. Adjacent lines differ in concentration by a factor of 10. u_z = 0.5 mm/yr. (Cases 3 and 5)

Figure 16. Effect of sorption on liquid-phase concentration of ^{99}Tc after transport through Yucca Mountain tuff at normal flow rate for 10,000 yr. Adjacent lines differ in concentration by a factor of 10. u_z = 0.5 mm/yr. (Cases 4 and 6)

Figure 17. Hypothesized model of the flow regime through the hydrogeologic units at Yucca Mountain.

GEOCHEMISTRY SIMULATION OF YUCCA MOUNTAIN: MODELING THE TRANSPORT OF URANIUM AND TECHNETIUM THROUGH THE UNSATURATED TUFFS

by

Gail A. Cederberg, L. Eric Greenwade, and Bryan J. Travis
Earth and Space Sciences Division

9003860 0514

ABSTRACT

In this report, preliminary baseline calculations for the transport of uranium and technetium through the unsaturated zone at Yucca Mountain, Nevada, are presented. Uranium is representative of those radionuclides with extremely long half-lives and high values of sorption coefficients. Technetium is representative of the most soluble and fastest moving radionuclides. First, a foundation for the calculations is discussed. This foundation, a referenced geochemical/geophysical model, contains the current stratigraphic, petrologic, hydrogeologic, geochemical, and material property data for the Yucca Mountain site. Second, the integrated transport of uranium and technetium from the repository to the water table is modeled. An expected-case flow scenario and an extreme-case flow scenario are used in the transport calculations. Because of the uncertainty associated with technetium sorption, the sorption of technetium is included and then neglected in both flow scenarios. Thus, six transport cases are modeled. Results show that the estimated uranium transport is only slightly sensitive to the magnitude of the flow because sorption has a significant effect on the retardation. The results for technetium transport closely resemble the results for uranium transport. The flow dominates the transport when sorption is neglected. Although the quantitative results using this preliminary model indicate that EPA requirements for a nuclear waste repository will be met easily, the model must be updated to a more realistic form before this conclusion can be regarded as dependable. These preliminary baseline calculations will be used as a basis to investigate the effects of physical and geochemical processes on the long-term transport of radionuclides at Yucca Mountain.

I. EXECUTIVE SUMMARY

An area containing unsaturated fractured tuffs at Yucca Mountain, Nevada, is one of the potential sites being considered for geologic storage of high-level radioactive waste. The Environmental Protection Agency (EPA) 40 CFR 191 Regulation limits the cumulative releases of many radionuclides from the repository to the accessible environment for 10,000 yr after disposal (U.S. EPA 1985). An estimate of the transport and retardation of radionuclides is necessary to assess the expected postclosure performance of a potential repository.

To satisfy this need, a continuing series of calculations is being carried out simulating the radionuclide transport from the repository to the accessible environment using the latest available models and data. These calculations will be used to investigate the effects of physical and geochemical processes on the long-term transport of radionuclides at Yucca Mountain. This report presents the results of a first set of calculations of radionuclide transport from the disturbed zone to the water table. The transport pathway is the unsaturated zone. The geochemical/geophysical model used in these calculations is a preliminary one; much more information is needed before the geochemical/geophysical model can be regarded as sufficiently complete so that it can be used for making dependable predictions.

The transport of two radionuclides is modeled: ^{234}U and ^{99}Tc. Uranium is representative of radionuclides with long half-lives and high values of sorption coefficients, and technetium is representative of the most soluble and fastest moving radionuclides. Two flow velocities through the tuff are used for each radionuclide and for each sorption condition: an expected average velocity of 0.5 mm/yr and an extreme average velocity of 4.5 mm/yr. Thus, six transport scenarios are modeled.

The following major conclusions were made from these simulations:

(1) For uranium, the estimated transport is only moderately sensitive to the magnitude of the flow. The insensitivity is caused by the sorptive properties of the tuffs of Yucca Mountain.

(2) For technetium, the sorption distribution coefficient is only slightly less than that for uranium in the repository unit, and the results for technetium transport closely resemble the results for uranium transport.

(3) Flow dominates the transport when sorption is negligible.

(4) The uranium, based on the preliminary geochemical/geophysical model, is not transported beyond the stratigraphic unit in which the repository is located in both the expected and extreme flow scenarios.

(5) The technetium, based on the preliminary geochemical/geophysical model and preliminary sorption data, is not transported beyond the stratigraphic unit in which the repository is located in both the expected and extreme flow scenarios.

(6) If technetium sorption is negligible, a measurable amount of it moves to the water table under conditions of high flow rate. Nevertheless, the amount of technetium transported to the water table, based on the preliminary geochemical/geophysical model, is still within the EPA-defined limits for a nuclear waste repository.

The following recommendations for future studies and data aquisition are made to better determine the significance and importance of processes affecting transport, to characterize the site more completely, and to assess expected postclosure performance of the potential repository.

(1) Many more data are needed before the geochemical/geophysical model of Yucca Mountain can be regarded as satisfactory and a suitable base for predictive simulations. Collection of these data should be a high priority.

(2) Since radionuclide transport is so sensitive to sorption, more sorption data are needed for radionuclide sorption on the various tuffs of Yucca Mountain, especially the stratigraphic units directly underlying the proposed repository.

(3) Additional simulations should be carried out coupled to more complex models of the flow paths and stratigraphy within Yucca Mountain.

II. INTRODUCTION

The Nevada Nuclear Waste Storage Investigations (NNWSI) Project is charged with studying the feasibility of placing a high-level nuclear waste repository in the volcanic tuffs beneath Yucca Mountain, Nevada. The mined geologic disposal system must meet the system performance objectives for radionuclide releases to the accessible environment as required by the EPA

9 0 3 8 6 0 5 1 6

40 CFR Part 191 (U.S. EPA 1985). To assess the expected postclosure performance of a potential repository, radionuclide transport and retardation estimates obtained from numerical simulations are necessary. One ongoing investigation in the NNWSI Project is to determine the significance and relative importance of the physical and geochemical processes affecting radionuclide transport. As one part of this specific investigation, the transport of uranium and technetium through the unsaturated zone has been modeled. The calculations presented in this report represent a simplest case scenario for radionuclide transport. These preliminary baseline calculations will serve as reference points for comparison with more complex, integrated transport calculations carried out as site characterization proceeds.

This report describes the modeling of the transport of uranium and technetium from the repository to the water table. Uranium is representative of those radionuclides with extremely long half-lives and high values of sorption coefficients (Kerrisk 1985). Technetium is representative of the most soluble and fastest moving radionuclides (Kerrisk 1985). Estimates of the transport were made under two flow conditions for both radionuclides and two sorption conditions for technetium. A total of six scenarios were modeled. These calculations were made using the computer code TRACR3D (Travis 1984). Input for the computer code comes from a comprehensive, referenced geochemical/geophysical model (Greenwade and Cederberg 1987); this model is discussed in Section III. The geochemical/geophysical model contains the current stratigraphic, petrologic, hydrogeologic, geochemical, and material property data for the Yucca Mountain site. Known repository data and estimated values for data that are unavailable are given. TRACR3D and the scenarios that were modeled are described in Section IV. Because of the unavailability of data and an incomplete understanding of all the processes involved, two flow scenarios are included: a possible expected vertical flow rate of 0.5 mm/yr and a potential extreme flow rate of 4.5 mm/yr (Montazer and Wilson 1984; Wilson 1985). Also included is an additional set of calculations in which zero sorption of ^{99}Tc is assumed for both flow scenarios. An extreme-case scenario for radionuclide transport from the repository to the water table occurs when the higher flow rate of 4.5 mm/yr and zero sorption of ^{99}Tc are combined in a single simulation. The results of these simulations are

presented in Section V. A discussion of the results is given in Section VI. Conclusions from this study and recommendations for future studies and data acquisition are given in Section VII.

III. GEOCHEMICAL/GEOPHYSICAL MODEL

Before any site-specific radionuclide transport is modeled, the current stratigraphic, petrologic, hydrogeologic, geochemical, and material data for that site should be collected. This section summarizes the data that were reported in a comprehensive, referenced geochemical/geophysical model (Greenwade and Cederberg 1987). The known repository data pertinent to the Yucca Mountain site were compiled, and unknown parameter values were estimated based on available data. As site characterization proceeds, this conceptual geochemical/geophysical model will be continually updated and revised to reflect the currently gathered information and data.

A. Stratigraphy

A stratigraphic model is used to divide the total transport path (i.e., from the repository to the water table) into geologically distinct units. The stratigraphy of the Yucca Mountain tuffs is quite complex. In general, there are alternating layers of welded and nonwelded tuffs. The geologic, hydrogeologic, and geochemical properties vary considerably among units. The variations are largely due to differences in the degree of welding of the tuffs and differences in material composition. These variations may significantly affect the overall estimated transport.

Figure 1 shows in a schematic form the general stratigraphy of Yucca Mountain (Greenwade and Cederberg 1987). The stratigraphic model given in Fig. 1 is located midway between wells USW H-5 and USW G-4 in Yucca Mountain (Fig. 5; from Ortiz et al. 1984). This location was selected because smaller relative error estimates associated with the elevations were given by kriging the values for the elevations obtained from drill hole data (Campbell 1986). Kriging is a geostatistical technique used to calculate minimum-variance, unbiased, linear estimates of parameters from measured data (Matheron 1963, 1971). The elevations used in this report were taken from the TUFF Data Base (TUFF 1986a) because the data base is very easy to access. In this case, the TUFF Data Base provides the same values for the elevations as those obtained by kriging (Campbell 1986). The zero elevation

is defined to be at the static water level (SWL), and the bottom of the potential repository slab is at an elevation of 257.69 m.

For the unsaturated zone, the mountain is broken into the following units, each with distinct thermal/mechanical properties (Ortiz et al. 1984): (1) TCw, Tiva Canyon welded; (2) PTn, Paintbrush nonwelded; (3) TSw, Topopah Spring welded; (4) CHn, Calico Hills nonwelded; (5) PPw, Prow Pass welded; and (6) CFUn, Upper Crater Flat nonwelded. The TSw unit is divided in three subunits, TSw1, TSw2, and TSw3. These three subunits have distinct material and sorptive properties (see Table II). The CHn unit is divided into four subunits. The first subunit, CHn1v, is a vitric layer. CHn1z is a zeolitic layer. CHn2 and CHn3 are both assumed to be zeolitic layers having distinct material properties.

B. Properties of the Geologic Media

The major properties and characteristics of the geologic media that affect transport are saturation, porosity, and dispersivity. The matrix bulk density also affects transport but only through the geochemistry process and the particular definition of equilibrium sorption used in this report. Values for saturation, porosity, and matrix bulk density for each of the subunits are given in Table I. The values listed in Table I are the unweighted means of drill hole data provided by the TUFF Data Base (TUFF 1986b, TUFF 1986c).

The dispersivity is often used to characterize the dispersion, or mixing and spreading of the plume caused by microscopic velocity variations within the pores (Bear 1972). In recent years, studies have suggested that dispersivity is not constant but rather depends on (1) the scale of local heterogeneities (e.g., fracture spacing or the spatial variability of hydraulic conductivity), (2) large-scale heterogeneities (e.g., distinct geologic units), and (3) the mean travel distance and/or scale of the system (Matheron and de Marsily 1980; Pickens and Grisak 1981; Gelhar and Axness 1983).

For the Yucca Mountain site, dispersivity data and general information concerning dispersion do not exist at this time. Minimum values for longitudinal and transverse dispersivity were chosen based on fracture spacing (Montazer and Wilson 1984), a scale of local heterogeneities. The effects

0 5 1 9 0 3 8 6

of flow and sorption are being investigated in this report, therefore, minimum dispersivity values were chosen so that the effects of dispersion would be negligible. The value for longitudinal dispersivity, a_L, was set to 10 cm, and the value for transverse dispersivity, a_T, was set to 1 cm. For these preliminary calculations, each stratigraphic unit was assigned the same values of longitudinal and transverse dispersivity.

C. Hydrogeology

Fluid flow at Yucca Mountain occurs through heterogeneous, anisotropic, fractured tuff. Little is known about the natural groundwater flow in the unsaturated zone, and investigations in this area are only in the preliminary stages (Montazer and Wilson 1984; Roulon et al. 1986). Analyses indicate that the distribution of the vertical percolation is nonuniform in the unsaturated zone (Montazer and Wilson 1984). Preliminary calculations (Roulon et al. 1986) indicate that because of the dip of the stratigraphic units and because of their hydraulic properties, a significant proportion of the flow above and/or below the proposed repository horizon may be diverted laterally into a permeable fault zone. The magnitude and location of the calculated lateral flow depend upon whether matrix-flow or fracture-flow conditions are assumed for the highly fractured units, upon the flux specified at the ground surface, and upon the hydraulic properties assigned to the fault zone. The results of these calculations are controlled by poorly known hydraulic parameters such as the characteristic curves (Roulon et al. 1986).

Although the stratigraphic analyses indicate the presence of tipped beds and early hydrologic studies indicate that the tipping may affect fluid flow, too little is known about these effects to incorporate them into our model at the present time. In this report, it is assumed that the recharge rate is applied as a constant vertical velocity field over the entire mountain. A simplest case scenario for simulating radionuclide transport occurs when a constant vertical velocity field is assumed. These preliminary calculations will serve as reference points for comparison with the more complex, integrated transport calculations carried out as site characterization proceeds and the hydrogeology is better understood. For all the stratigraphic units, the flow is presumed to be matrix dominated with insignificant lateral or fracture flow. An expected value for u_z, the

average vertical flow rate, is 0.5 mm/yr, whereas an extreme value may be as high as 4.5 mm/yr (Montazer and Wilson 1984; Wilson 1985).

D. Geochemistry

The main geochemical processes affecting transport are sorption and molecular diffusion. One parameter that can be associated with equilibrium sorption is the distribution coefficient, K_d (cm^3/g), and the parameters associated with molecular diffusion are the diffusion coefficient, D (cm^2/s), and the constrictivity, τ_c. The distribution coefficient is a measure of the partitioning of a solute between the solid- and aqueous-phase under conditions of local equilibrium. The following equation gives the relationship between the solid and aqueous-phase concentrations for the distribution coefficient sorption model:

$$\bar{C} = K_d C, \qquad (1)$$

where

$\bar{C}$ ≡ sorbed-phase concentration, (g/g);
K_d ≡ equilibrium distribution coefficient, (cm^3/g);
C ≡ aqueous-phase concentration, (g/cm^3).

The larger the value of K_d, the more solute is sorbed onto the solid phase. For both aqueous- and solid-phase concentrations, in g/total cm^3 of fluid, $\bar{C} = (K_d C)(\rho/\epsilon\sigma)$.

Molecular diffusion causes mixing of the contaminants in the fluid because each solute has its own pathline with respect to the flow domain as well as its own velocity along that pathline. The transport time between points of interest will be lengthened if the flow velocity is relatively small so that enough time exists for a significant portion of the radionuclide to diffuse into the fluid in the surrounding matrix material. In this report, constrictivity is considered to be a combination of two factors: the measure of the deviation of the pathline of transport from a straight path (the standard definition of tortuosity), and the narrowing of the pores, usually called constrictivity. For most real porous systems, it is impossible to separate the two factors (Satterfield 1970). It is also this combined quantity that is determined experimentally.

Experimentally determined (Thomas 1986) and extrapolated values (Greenwade and Cederberg 1987) for apparent distribution coefficients, K_d's, are given in Table II for the radionuclides ^{99}Tc and ^{238}U. They are called apparent distribution coefficients to acknowledge the fact that the reaction in the laboratory may not have reached a state of reversible equilibrium (Thomas 1986). In Table II, values based on the experimental K_d data were assigned to the appropriate thermal/mechanical unit by correlating the depths of the samples (Thomas 1986) with the stratigraphic information (Ortiz et al. 1984). As a first approximation, the unweighted mean was taken of all the data for a particular unit regardless of the drill hole from which the sample had originated. Where data were unavailable, distribution coefficient data were assigned to stratigraphic units based on the unit's mineral composition (Thomas 1986) and material type (Broxton 1985; 1986). Details are given in a recent report (Greenwade and Cederberg 1987). Investigations to further characterize the mineral compositions of the stratigraphic units are being done at Los Alamos (Broxton 1986). An observation in Table II is that the distribution coefficient for technetium is non-zero in several stratigraphic units. This is important because it is usually assumed that technetium exhibits little sorption, much less than observed experimentally in the TSw2 unit (Tien et al. 1985).

Values for the molecular diffusivity coefficients for uranium and technetium were not available from the results of current Los Alamos investigations (Rundberg 1986) or from the literature. Therefore, D is set equal to 1.5×10^{-5} cm^2/s based on an expected value of 1.46×10^{-5} cm^2/s for an element such as technetium (Rundberg 1986). This is consistent with values for other materials, as diffusion coefficients for substances diffusing through bulk water are normally around 10^{-5} cm^2/s (Reid et al. 1977). Values for the constrictivity coefficients were obtained from the results of diffusion cell experiments (Rundberg 1986). For the welded units, τ_c = 0.037, and for the nonwelded units, τ_c = 0.030.

E. Source Term

Another area of active investigation in the NNWSI Project is estimating a source term for the radionuclides based on factors such as waste package design and volume of water intercepting the waste package. This work is principally being done at Lawrence Livermore National Laboratory (Oversby

1986). Preliminary estimates of the source terms for technetium and uranium are $C_o[^{99}Tc] = 2.6 \times 10^{-8}$ g/cm^3 (Oversby and Wilson 1986) and $C_o[^{233}U] = 5.0 \times 10^{-6}$ g/cm^3 (Oversby 1986). In the transport calculations that were carried out for this report, the values given above were used as constant-concentration sources of the radionuclides.

IV. NUMERICAL SIMULATIONS

A. TRACR3D

The TRACR3D code (Travis 1984) was used to perform the transport calculations discussed in Section V. TRACR3D solves the equations of transient two-phase flow and multi-component transport in deformable, heterogeneous, reactive porous/fractured media. The code uses an implicit finite-difference technique to solve the flow equations and a semi-implicit finite-difference method to solve the transport equations. One-, two-, or three-dimensional grids can be used in either Cartesian or cylindrical coordinates. Verification of the TRACR3D transport model was carried out by comparing TRACR3D with five analytic solutions to problems involving tracer transport (Travis 1984). It was shown that TRACR3D can accurately solve the model equations. Validation of the TRACR3D transport model was demonstrated by comparing simulation results with the results of several experiments. Two experiments that have application to transport at Yucca Mountain are (1) diffusion of a sorbing tracer from a well-stirred solution into a thin wafer of tuff and (2) migration of radioactive tracers from an underground nuclear test to a nearby well as a result of pumping in the well. The model and experimental results were in very good agreement (Travis 1984).

For the simulations presented in this report, the equation of mass transport for each radionuclide is given by

$$\partial_t(\varepsilon\sigma\rho C) + \nabla\cdot(\rho\vec{u}C) = \nabla\cdot(\varepsilon\sigma\tau_c D\rho\nabla C) + \nabla\cdot[\varepsilon\sigma\bar{\bar{D}}\nabla(\rho C)] - \varepsilon\lambda\sigma\rho C - \rho\rho_m K_d(\partial_t C + \lambda C), \quad (2)$$

where

∂_t ≡ partial derivative with respect to time;
ϵ ≡ porosity, volume of voids/total volume;
σ ≡ saturation, volume of fluid/volume of voids;
ρ ≡ fluid density, g/cm^3;
$\vec{u}$ ≡ average pore water velocity vector, cm/s;
C ≡ radionuclide concentration, g radionuclide/g fluid;
τ_c ≡ constrictivity, dimensionless;
D ≡ molecular diffusivity of radionuclide, cm^2/s;
$\bar{D}$ ≡ hydrodynamic dispersion tensor, cm^2/s;
λ ≡ ln(2)/half-life of radionuclide, 1/s;
ρ_m ≡ matrix bulk density, g/cm^3;
K_d ≡ equilibrium distribution coefficient, cm^3/g.

The processes modeled in Eq. 2 are advection, molecular diffusion, mechanical dispersion, radionuclide decay, and equilibrium sorption. For this report, the TRACR3D model is used in its two-dimensional configuration. The simulations were computed in the z, the vertical direction, and x, the horizontal direction. Because we are considering one-dimensional flow in the downward vertical direction, $\vec{u} = u_z$. Therefore, $D_{zz} = \alpha_L u_z$, and $D_{xx} = \alpha_T u_z$ (Bear 1972). Tables I and II give the values for ϵ, σ, ρ_m, and K_d for each of the stratigraphic units.

In the calculations that were carried out for this study, two constant concentration radionuclide line sources, each 0.25 m wide, were placed 30 m apart. The zone sizes, or grid spacings, in the horizontal direction were increased from 0.25 m to 2 m as one moved away from the sources. The finer grid spacings near the sources allowed the region near the source to be well characterized. In the horizontal direction, 52 zones were used to model the total horizontal distance, 72.75 m. This horizontal distance was chosen so that spreading of the radionuclide plume due to lateral dispersion would be modeled and included in the results. In the vertical direction, 130 zones were used to model the distance from the line source to the water table, 265.4 m. This number of vertical zones was chosen so that the number of subdivisions per stratigraphic unit provided a vertical cell size of approximately 2.5 m. The actual minimum and maximum zone sizes in the vertical direction were 2.416 m and 2.786 m, respectively. Test problems were run on

0 5 2 4 0 3 8 6

the CRAY XMP computer to investigate the effects of zone sizes on the accuracy of the results. The zone sizes given above were selected because further refinement of the zones resulted in little if any changes in the numerical answers.

B. Scenarios

The transport of uranium and technetium from the repository to the water table was modeled by using the geochemical/geophysical model discussed in Section III as a basis. Uranium is representative of those radionuclides that have longer half-lives and are more reactive with the porous media. Technetium is representative of those radionuclides that are relatively more soluble and less reactive with the porous media. In the calculations, two radionuclide line sources of constant concentration were used.

To investigate the effects of flow on transport, two flow scenarios were included: a possible expected vertical velocity, 0.5 mm/yr, and a potential extreme velocity, 4.5 mm/yr. Because of the unavailability of data and an incomplete understanding of the technetium sorption process, additional calculations were made which neglected ^{99}Tc sorption in all the stratigraphic units [i.e., $K_d(^{99}Tc) = 0$]. Table III lists the six transport cases examined in this report. The results from Case 3 are compared with those of Case 5 and the results of Case 4 are compared with those of Case 6 to investigate the effects of sorption on transport. The results from Case 1 are compared with those of Case 2, the results from Case 3 are compared with those of Case 4, and the results from Case 5 are compared with those of Case 6 to investigate the effects of flow on transport. Case 6 represents an extreme-case scenario for radionuclide transport from the repository to the water table. The extreme-case scenario has the higher flow rate of 4.5 mm/yr and zero sorption of ^{99}Tc.

V. RESULTS

A. Uranium Transport

Figures 2 and 3 show the results of simulating the Case 1 scenario (^{238}U transport; u_z = 0.5 mm/yr). Figure 2 presents the logarithmic concentration profiles of aqueous-phase ^{238}U. Figure 3 shows the logarithmic concentration profiles of solid-phase ^{238}U (i.e., the concentration of ^{238}U

sorbed onto the tuff). Profiles at times of approximately 5,000, 10,000, and 15,000 yr are shown. The leading edge of the ^{238}U plume migrated approximately 20 m in 10,000 yr. In the paragraphs that follow, the leading edge of the plume is defined as the line with a concentration of 10^{-11} g radionuclide/cm^3 of liquid. At 10,000 and 15,000 yr, the aqueous- and sorbed-phase ^{238}U remained in the TSw2 unit and had not migrated into the Tuff of Calico Hills.

Figures 4 and 5 show the results of simulating the Case 2 scenario (^{238}U transport; u_z = 4.5 mm/yr). Figure 4 presents the logarithmic concentration profiles of aqueous-phase ^{238}U. Figure 5 shows the logarithmic concentration profiles of solid-phase ^{238}U. Profiles at times of approximately 5,000, 10,000, and 15,000 yr are shown. In this case, under the condition of an extreme flow rate, the leading edge of the ^{238}U plume migrated approximately 40 m in 10,000 yr. At 10,000 and 15,000 yr, the aqueous- and sorbed-phase ^{238}U remained contained in the TSw2 unit and had not migrated into the Tuff of Calico Hills.

Figure 6 presents a comparison of the results of the ^{238}U transport calculations at 10,000 years for both flow scenarios (Cases 1 and 2). In Case 2 where the flow velocity is set at a potential extreme value, the leading edge of the plume has migrated through the repository only 20 m more than in Case 1. The increase in the flow by a factor of 9 (almost an order of magnitude) resulted in only a factor of 2 increase in the distance the leading edge of the ^{238}U plume migrated. The simulated distance the plume migrated was only slightly sensitive to the magnitude of the average flow. In the case of uranium transport, equilibrium sorption had a more significant effect in controlling the long-term transport. In the TSw2 unit, $K_d(^{238}U)$ was estimated to be 2.84 cm^3/g. This implies that for every 10 units of uranium in the aqueous phase, there will be approximately 60 units of uranium sorbed onto the tuff (see Eq. 1).

B. Technetium Transport

Figures 7 and 8 show the results of simulating the Case 3 scenario (^{99}Tc transport; u_z = 0.5 mm/yr; sorption). Figure 7 presents the logarithmic concentration profiles of aqueous-phase ^{99}Tc. Figure 8 shows the logarithmic concentration profiles of solid-phase ^{99}Tc. Profiles at times of approximately 5,000, 10,000, and 15,000 yr are shown. The leading edge of

the ^{99}Tc plume had migrated approximately 25 m at 10,000 yr. Under the condition of an expected flow rate of 0.5 mm/yr, the aqueous- and sorbed-phase ^{99}Tc plumes remained in the TSw2 unit and did not migrate into the Tuff of Calico Hills. The results for ^{99}Tc transport closely resemble the ^{238}U transport results simulated using the low flow scenario (see Fig. 2).

Figures 9 and 10 show the results of simulating the Case 4 scenario (^{99}Tc transport; u_z = 4.5 mm/yr; sorption). Figure 9 presents the logarithmic concentration profiles of aqueous-phase ^{99}Tc. Figure 10 shows the logarithmic concentration profiles of solid-phase ^{99}Tc. Profiles at times of approximately 5,000, 10,000, and 15,000 yr are shown. The leading edge of the ^{99}Tc plume had migrated approximately 65 m at 10,000 yr and remained within the TSw2 unit. It is interesting to note the behavior of ^{99}Tc at 15,000 yr. At 15,000 yr, the ^{99}Tc plume had migrated into the Chn1z unit, approximately 125 m below the source. Below the TSw2 unit, the plume does not exhibit the extent of the lateral spreading observed in the TSw2 unit. The values for distribution coefficients for the units underlying TSw2 are 0.0 in TSw3, 0.04 in CHn1v, and 0.0098 in CHn1z (see Table II). Sorption has an negligible effect on transport in these units. However, Fig. 10 does show a sorbed-phase concentration of ^{99}Tc in the CHn1v unit where K_d = 0.04 cm^3/g. Compared with the low flow scenario where the results of ^{99}Tc and ^{238}U transport closely resembled each other, in the extreme flow scenario, the ^{99}Tc plume migrated 25 m farther than did the ^{238}U plume. As the flow rate is increased, sorption becomes a less dominant mechanism in controlling transport.

Figure 11 presents a comparison of the results of the ^{99}Tc transport calculations at 10,000 yr for both flow scenarios when sorption is considered (Cases 3 and 4). In Case 4 where the flow velocity is set at a potentially extreme value, the leading edge of the plume has migrated through the repository 40 m more than in Case 3. An increase in the flow by a factor of 9 (almost an order of magnitude) resulted in an increase in the distance the leading edge of the ^{99}Tc plume migrated by a factor of three. The simulated distance the plume migrated was moderately sensitive to the magnitude of the average flow.

Figure 12 shows the results of simulating the Case 5 scenario (^{99}Tc transport; u_z = 0.5 mm/yr; no sorption). Although Cases 5 and 6 may not

represent actual system behavior for ^{99}Tc, there is still uncertainty associated with the sorption behavior of ^{99}Tc in the TSw2 unit (Thomas 1986). The results from this simulation and the results from Case 6 are representative of the transport of conservative, nonsorbing radionuclides and are helpful in examining the effect of sorption on transport. Figure 12 presents the logarithmic concentration profiles of aqueous-phase ^{99}Tc. Profiles at times of approximately 5,000, 10,000, and 15,000 yr are shown. At 10,000 yr, the leading edge of the ^{99}Tc plume migrated out of the repository unit and into the CHnlv unit, approximately 100 m below the source.

Figure 13 shows the results of simulating the Case 6 scenario (^{99}Tc transport; u_z = 4.5 mm/yr; no sorption). Case 6 represents an extreme-case transport scenario where the higher flow rate, 4.5 mm/yr, and zero sorption of ^{99}Tc are combined in one simulation. Figure 13 presents the logarithmic concentration profiles of aqueous-phase ^{99}Tc. Profiles at times of approximately 5,000 and 10,000 yr are shown. At 10,000 yr, the leading edge of the ^{99}Tc plume migrated through the entire unsaturated zone into the CFUn unit and reached the static water level, totaling a distance of approximately 300 m.

The only case in which any calculated amount of radionuclide was transported to the water table was Case 6. In Case 6, approximately 1.6×10^{-5} gm (2.8×10^{-7} Ci) of ^{99}Tc/two sources was estimated to have accumulated below the static water table in the groundwater at 10,000 yr. For one line source, this equals 1.4×10^{-7} Ci/source. The allowable cumulative release to the accessible environment for 10,000 yr after disposal is 10,000 Ci of ^{99}Tc per 1000 MTHM (metric tons of heavy metal) exposed to a burnup between 25,000 and 40,000 megawatt-days/MTHM (U.S. EPA 1985). If there are 70,000 MTHM in the inventory (p. 6-365, U.S. EPA 1985) or 27,000 canisters each containing 2.59 MTHM in the potential repository, then the EPA allowable cumulative release would be 700,000 Ci of ^{99}Tc in 10,000 yr. Given the conditions of Case 6, assuming one line source represents a canister, and assuming all the 27,000 canisters in the repository were to be breached, the total curie load to the water table would be 3.8×10^{-3} Ci, less than 10^{-8} (or one hundred millionth) of the allowable EPA containment requirement.

Figure 14 presents a comparison of the results of the ^{99}Tc transport calculations at 10,000 yr for both flow scenarios when sorption is neglected

0 0 3 8 6 0 5 2 8

(Cases 5 and 6). In Case 6 where the flow velocity is set at a potential extreme value, the leading edge of the plume has migrated through the repository 200 m more than in Case 5. An increase in the flow by a factor of 9 resulted in an increase in the distance the leading edge of the ^{99}Tc plume migrated by a factor of 3. In this comparison where sorption is zero, the simulated distance the plume migrated was moderately sensitive to the magnitude of the average flow. Advection is the controlling transport process.

C. Effects of Sorption

The effects of sorption on the transport of radionuclides can be examined by comparing Case 3 with Case 5 and Case 4 with Case 6. Figure 15 shows the comparison of results of the transport calculations for ^{99}Tc at approximately 10,000 yr for Cases 3 and 5. The same flow scenario, 0.5 mm/yr, is used in the two cases but in Case 5 zero sorption of ^{99}Tc is assumed. In Case 3, the ^{99}Tc plume remains within the TSw2u unit. In Case 5, the leading edge of the plume migrated into the CHnlv unit, 80 m (a factor of 4) farther than did the plume in Case 3. Also note the increased lateral spreading in Case 5, which is due to lateral dispersion.

Figure 16 shows the results of transport calculations for ^{99}Tc at approximately 10,000 yr for Cases 4 and 6. The same flow scenario, 4.5 mm/yr, is used in the two cases but in Case 6 zero sorption of ^{99}Tc is assumed. In Case 4, the ^{99}Tc plume migrated 60 m and remained within the TSw2 unit. In Case 6, the leading edge of the plume reached the static water level, migrated into the CFUn unit, traveling 230 m (a factor of 4) farther than did the plume in Case 4.

In these expected- and extreme-case flow scenarios, the estimated ^{99}Tc transport was very sensitive to the degree of sorption. In both comparisons, when sorption was zero the leading edge of the plume traveled a factor of 4 farther. Sorption can be a significant retarding mechanism when the flow is at either a relatively low or high level.

D. Effects of Flow

The effects of flow on the transport of radionuclides can be summarized by comparing Case 1 with Case 2 (Fig. 6), Case 3 with Case 4 (Fig. 11), and Case 5 with Case 6 (Fig. 14). These comparisons were described in detail in the previous sections. In these three sets, the sorption was held constant in each set and the flow was changed from 0.5 mm/yr to 4.5 mm/yr. In Fig. 6, the increase in the flow by a factor of 9 resulted in a factor of 2 increase in the distance the leading edge of the ^{238}U plume migrated. The actual difference in distance migrated was 20 m. In Fig. 11, the leading edge of the ^{99}Tc plume migrated 40 m more (approximately a factor of 3) when the higher flow scenario and sorption were considered. In Fig. 14, the leading edge of the ^{99}Tc plume migrated 200 m more (a factor of 3) when the higher flow scenario was considered and sorption was neglected. As the amount of sorption decreased from comparison to comparison (^{238}U, Fig. 6; ^{99}Tc with sorption, Fig. 11; ^{99}Tc zero sorption, Fig. 14), the actual difference in distance the leading edge of the plume migrated increased. When sorption is a significant controlling transport process as in the case of ^{238}U transport, the transport is only slightly sensitive to an increase in flow. When sorption becomes less significant, the transport becomes more and more sensitive to an increase in the flow.

VI. DISCUSSION

A. Geochemical/Geophysical Model

As the Yucca Mountain site is more fully characterized in future investigations, the geochemical/geophysical model will be updated and revised. Several important areas need to be addressed. The stratigraphic model for the transport calculations should include the 5 to 10 degree eastward tilt (Ortiz et al. 1984) of the tuffs and explicit faults. Geologic faults need to be included so a more accurate model of potential transport pathways can be provided. In a recent report (Roulon et al. 1986) it was shown that lateral flow caused by the tipped beds occurred under both matrix and fracture flow conditions. The tipped beds and geologic faults were not included at this time because of the unavailability of data concerning the natural groundwater flow and fault parameters.

A better understanding of the natural groundwater flow in each of the stratigraphic units is needed. Work in this area is also in preliminary stages (Roulon et al. 1986). Figure 17 shows a hypothesized model of the flow regime through the hydrogeologic units at Yucca Mountain. If indeed a portion of the flow is diverted laterally around the Tuff of Calico Hills and into a much more permeable fault zone, the groundwater travel time to the accessible environment could be decreased and radionuclide releases could be increased.

There is a general unavailability of data for most of the parameters that describe the geologic media. Much of the available data is extremely localized around the drill holes where the core samples were collected. Some type of data analysis, such as kriging, should be done on parameters such as saturation, porosity, and bulk density. Values for those parameters could then be extrapolated to locations away from the drill holes, and estimates of error could be assigned to the estimated parameter values.

Because sorption plays such an important role in the overall estimated transport, more sorption data related to the units directly underlying the repository should be collected. Also, more information is needed on the errors associated with the experimentally determined distribution coefficients. More specific geochemistry should be investigated such as the geochemical species present, thermodynamic formation constants for aqueous and sorbed species, and alternative sorption models (e.g, isotherms and non-equilibrium sorption models).

Unless it can be shown that data can be inferred with a high degree of confidence, less uncertain and more material and geochemical data should be gathered. In some cases, much data exist within one layer, but none exist within the next layer. As demonstrated with the sorption data, several stratigraphic units had no associated values of distribution coefficients.

B. Transport Calculations

As the geochemical/geophysical model is updated and revised, the baseline transport calculations will also be updated. The best available set of transport estimates is needed as a baseline from which to further investigate the effects and significance of the geochemical and geophysical processes controlling transport.

900385 0531

In particular, as the natural groundwater flow becomes better understood, more complex flow models need to be incorporated into the transport calculations. Lateral flow and possible flow through more permeable fault zones should be added. If flow is diverted laterally to a fault, the transport path to the accessible environment may be shortened and cumulative radionuclide releases may be increased. The transport should be estimated at other locations within Yucca Mountain. In other locations, the distance to the water table is much less than in the examples presented here, and the material unit properties may differ (Ortiz et al. 1984).

The effects of dispersion on the cumulative radionuclide release should also be investigated. Dispersion is responsible for the mixing and spreading of the plume caused by microscopic velocity variations within the pores and by large-scale heterogeneities within the geologic media. The dispersivity in these examples was set to a minimum value. However, as the dispersivity increases, one might expect an increase in the cumulative release caused by a greater spreading of the radionuclides in the direction of flow.

In summary, the calculations presented in this paper are preliminary in nature and serve principally as one example of how radionuclide transport can be investigated. Before results of these calculations can be used in judging the suitability of the site for nuclear waste disposal, several factors need to be addressed. First, an accurate and referenced foundation for any set of transport calculations should be compiled. The availability and reliability of the data should be assessed. Areas where more data are required should be brought to the attention of other investigators. Finally, the results of many scenarios should be examined to isolate the effects of any one physical or geochemical process affecting transport.

VII. CONCLUSIONS AND RECOMMENDATIONS

This report presents the results of a first set of calculations of radionuclide transport from the disturbed zone to the water table. The transport pathway is the unsaturated zone. The geochemical/geophysical model used in these calculations is a preliminary one; much more information is needed before the geochemical/geophysical model can be regarded as sufficiently complete so that it can be used for making dependable predictions.

0 5 3 2 9 0 3 8 6

The transport of two radionuclides is modeled: ^{233}U and ^{99}Tc. Uranium is representative of radionuclides with long half-lives and high values of sorption coefficients, and technetium is representative of the most soluble and fastest moving radionuclides. Two flow velocities through the tuff are used for each radionuclide and for each sorption condition: an expected average velocity of 0.5 mm/yr and an extreme average velocity of 4.5 mm/yr. Thus, six transport scenarios are modeled.

A. Conclusions

The following major conclusions were made from these simulations:

(1) For uranium, the estimated transport is only moderately sensitive to the magnitude of the flow. The insensitivity is caused by the sorptive properties of the tuffs of Yucca Mountain.

(2) For technetium, the sorption distribution coefficient is only slightly less than that for uranium in the repository unit, and the results for technetium transport closely resemble the results for uranium transport.

(3) Flow dominates the transport when sorption is negligible.

(4) The uranium, based on the preliminary geochemical/geophysical model, is not transported beyond the stratigraphic unit in which the repository is located in both the expected and extreme flow scenarios.

(5) The technetium, based on the preliminary geochemical/geophysical model and preliminary sorption data, is not transported beyond the stratigraphic unit in which the repository is located in both the expected and extreme flow scenarios.

(6) If technetium sorption is negligible, a measurable amount of it moves to the water table under conditions of high flow rate. Nevertheless, the amount of technetium transported to the water table, based on the preliminary geochemical/geophysical model, is still within the EPA-defined limits for a nuclear waste repository.

B. Recommendations

The following recommendations for future studies and data aquisition are made to better determine the significance and importance of processes affecting transport, to more fully characterize the site, and to assess expected postclosure performance of the potential repository.

(1) Many more data are needed before the geochemical/geophysical model of Yucca Mountain can be regarded as satisfactory and a suitable base for predictive simulations. Collection of these data should be a high priority.

(2) Since radionuclide transport is so sensitive to sorption, more sorption data are needed for radionuclide sorption on the various tuffs of Yucca Mountain, especially the stratigraphic units directly underlying the proposed repository.

(3) More information is needed on the uncertainties associated with material property data and sorption coefficients.

(4) Some type of data analysis (e.g., kriging) should be done on the saturation, porosity, and sorption coefficient data.

(5) The effects of dispersion and matrix and/or fracture flow on transport should be investigated.

(6) Additional transport simulations coupled to more complex models of the flow paths and stratigraphy within Yucca Mountain should be carried out.

REFERENCES

Bear, J., 1972, Dynamics of Fluids in Porous Media, American Elsevier, New York, 1972, pp. 579-617.

Broxton, D. E., 1985, "Chemical Variability of Zeolites at a Potential Nuclear Waste Repository, Yucca Mountain, Nevada," presented at the International Symposium on Management of Hazardous Chemical Waste Sites, Winston-Salem, NC.

Broxton, D. E., 1986, Private Communication, Los Alamos National Laboratory, Los Alamos, NM.

Campbell, K., 1986, "Kriging for Interpolation of Sparse and Irregularly Distributed Geologic Data," NNWSI Milestone 376, Los Alamos National Laboratory, Los Alamos, NM.

Gelhar, L. W., and C. L. Axness, 1983, "Three-Dimensional Stochastic Analysis of Macrodispersion in Aquifers," Water Resources Research 19(1), 161-183.

Greenwade, L. E., and G. A. Cederberg, 1987, "Preliminary Geochemical/Geophysical Model of Yucca Mountain," NNWSI Milestone R343, Los Alamos National Laboratory, Los Alamos, NM.

Kerrisk, J. F., 1985, "An Assessment of the Important Radionuclides in Nuclear Waste," Los Alamos National Laboratory report LA-10414-MS, Los Alamos, NM.

Matheron, G., 1963, "Principles of Geostatistics," Econ. Geol. 58, 1246-1266.

Matheron, G., 1971, The Theory of Regionalized Variables and Its Applications, Ecole des Mines, Fontainebleau, France.

Matheron, G., and G. de Marsily, 1980, "Is Transport in Porous Media Always Diffusive? A Counterexample," Water Resources Research 16(5), 901-917.

Montazer, P., and W. E. Wilson, 1984, "Conceptual Hydrological Model of Flow in the Unsaturated Zone, Yucca Mountain, Nevada," Water-Resources Investigations Report 84-4345, U.S. Geological Survey, Lakewood, CO.

Ortiz, T. S., R. L. Williams, F. B. Nimick, B. C. Whittet, and D. L. South, 1984, "A Three-Dimensional Model of Reference Thermal/Mechanical and Hydrological Stratigraphy at Yucca Mountain, Southern Nevada," Sandia National Laboratories report SAND84-1076, Albuquerque, NM.

Oversby, V. M., 1986, Private Communication, Livermore National Laboratory, Livermore, CA.

Oversby, V. M., and C. N. Wilson, 1986, "Derivation of a Waste Package Source Term for NNWSI from the Results of Laboratory Experiments," Proceedings of the Symposium on the Scientific Basis of Nuclear Waste

Management IX, Stockholm, Sweden, Materials Research Society, Pittsburgh, PA, pp. 337-346.

Pickens, J. F., and G. E. Grisak, 1981, "Scale-dependent Dispersion in a Stratified Granular Aquifer," Water Resources Research 17(4), 1191-1211.

Reid, R. C., J. M. Prausnitz, and T. K. Sherwood, 1977, Properties of Gases and Liquids, 3rd ed., McGraw Hill, New York, pp. 576-577.

Roulon, J. G., S. Bodvarsson, and P. Montazer, 1986, "Preliminary Numerical Simulations of Groundwater Flow in the Unsaturated Zone, Yucca Mountain, Nevada," Lawrence Berkeley Laboratory report LBL-20553, Berkeley, CA.

Rundberg, R. S., 1986, Private Communication, Los Alamos National Laboratory, Los Alamos, NM.

Satterfield, C. N., 1970, Mass Transfer in Heterogeneous Catalysis, M.I.T. Press, Cambridge, Massachusetts, pp. 33-41.

Tien, P., M. D. Siegel, C. D. Updegraff, K. K. Wahi, R. V. Guzowski, 1985, "Repository Site Data Report for Unsaturated Tuff, Yucca Mountain, Nevada," Sandia National Laboratories report Sand84-2668, Albuquerque, NM.

Thomas, K. W., 1986, "A Summary Report on Sorption Measurements Performed with Yucca Mountain Tuff Samples and Water from Well J-13," NNWSI Milestone M313, Los Alamos National Laboratory, Los Alamos, NM.

Travis, B. J., 1984, "TRACR3D: A Model of Flow and Transport in Porous/Fractured Media," Los Alamos National Laboratory report LA-9667-MS, Los Alamos, NM.

TUFF Data Base Product #CAL0104, 1986a, Sandia National Laboratories, Albuquerque, NM.

TUFF Data Base Product #5, 1986b, Sandia National Laboratories, Albuquerque, NM.

TUFF Data Base Product #4, 1986c, Sandia National Laboratories, Albuquerque, NM.

U. S. Environmental Protection Agency, 1985, "40 CFR Part 191: Environmental Standards for the Management and Disposal of Spent Nuclear Fuel, High-Level and Transuranic Radioactive Wastes," AH-FRL2870-3, Washington, DC.

Wilson, W. E., 1985, "Unsaturated-Zone Flux at Yucca Mountain, Nevada," letter from W. E. Wilson (U.S. Geologic Survey, Denver, CO) to D. L. Vieth (WMPO, Las Vegas, Nevada), December 24, 1985.

Table 1

Material Properties of Stratigraphic Units

Unit	Saturation[a] σ	Porosity[b] ε	Bulk Density[b] ρ_m (g/cm^3)
TCw	0.86141	NA	2.2497
PTn	0.82410	NA	1.4211
TSw1	0.81527	0.11681	2.1672
TSw2	0.88568	0.11681	2.2629
TSw3	0.75876	0.11681	2.2953
CHn1v	0.85976	0.35405	1.5339
CHn1z	0.88960	0.30636	1.5910
CHn2	0.91438	0.30636	1.7750
CHn3	0.94008	0.30636	1.4800
PPw	0.84744	0.25274	1.8782
CFUn	0.92025	0.32393	1.6391

a. TUFF 1986b
b. TUFF 1986c

-900386 0537

Table II

Available and Estimated Distribution Coefficients, K_d's, for Yucca Mountain Tuffs

Unit	Tc (cm^3/g)		U (cm^3/g)	
	Available[a]	Estimated[b]	Available[a]	Estimated[b]
TCw		0.346		2.84
PTn	0.006		5.90	
TSw1	0.159		0.75	
TSw2	0.72			2.84
TSw3	0.00		0.00	
CHn1v	0.04		0.00	
CHn1z	0.0098		5.33	
CHn2		0.0098	12.0	
CHn3		0.0098		6.75
PPw		0.346	2.4	
CFUn	0.181		4.03	

a. Thomas 1986
b. Greenwade and Cederberg 1987

Table III

Scenarios for the Numerical Simulations of Uranium and Technetium Transport

Case	Radionuclide	Flow Velocity	Sorption
1	^{238}U	0.5 mm/yr	yes
2	^{238}U	4.5 mm/yr	yes
3	^{99}Tc	0.5 mm/yr	yes
4	^{99}Tc	4.5 mm/yr	yes
5	^{99}Tc	0.5 mm/yr	no
6	^{99}Tc	4.5 mm/yr	no

31 0 5 4 0 7 0 3 9 6

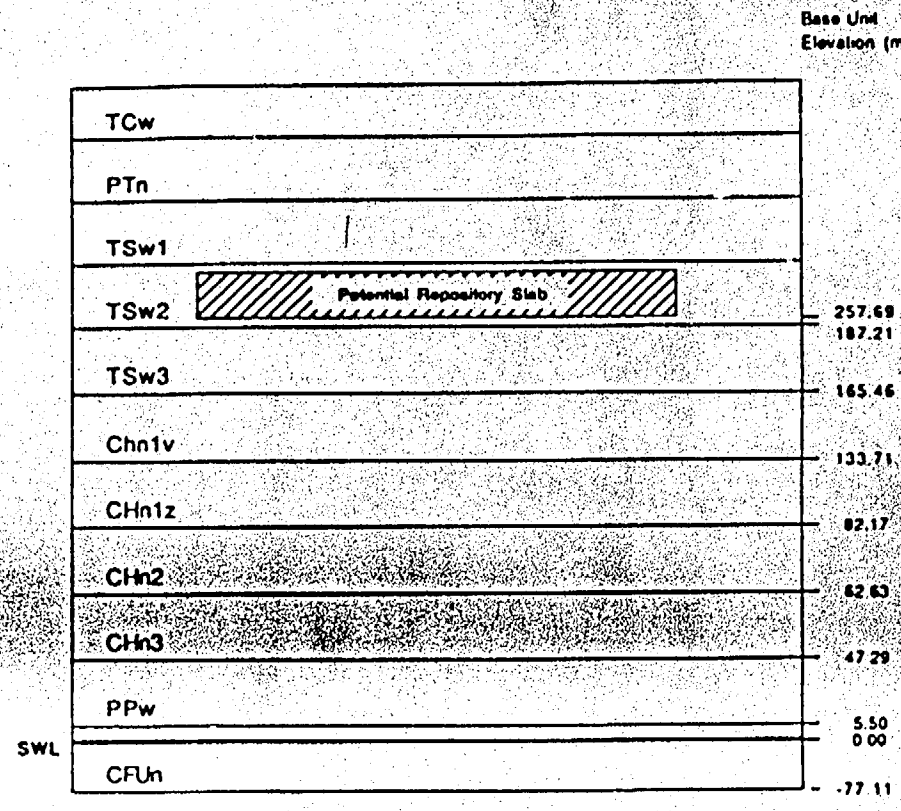

Figure 1. Schematic representation of Yucca Mountain stratigraphy (not to scale).

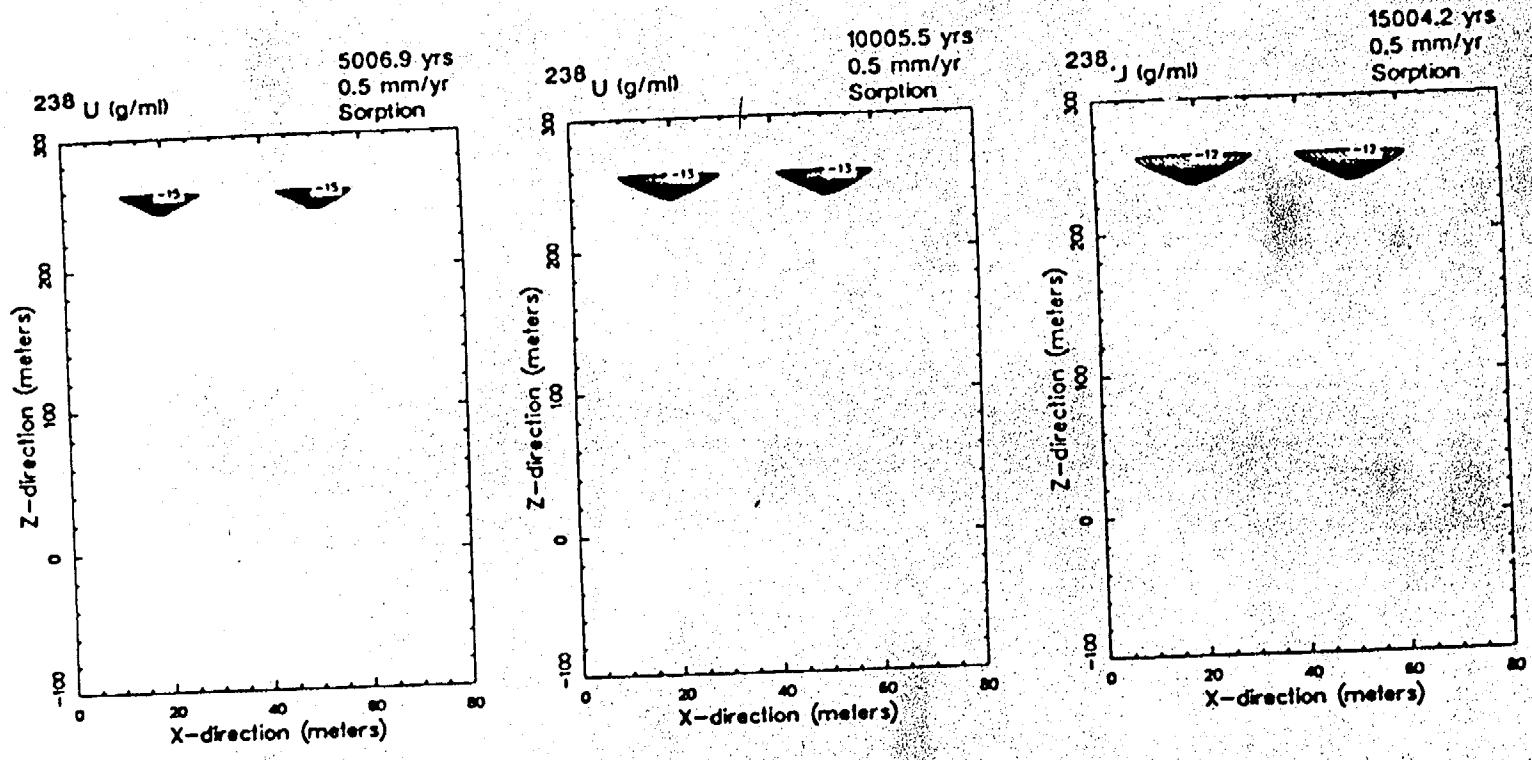

Figure 2. Liquid-phase concentrations during transport of ^{238}U through unsaturated Yucca Mountain tuff at normal flow rate. Adjacent lines differ in concentration by a factor of 10. u_z = 0.5 mm/yr. t = 5000, 10000, and 15000 yr. (Case 1)

0 5 4 1
2 0 3 8 6

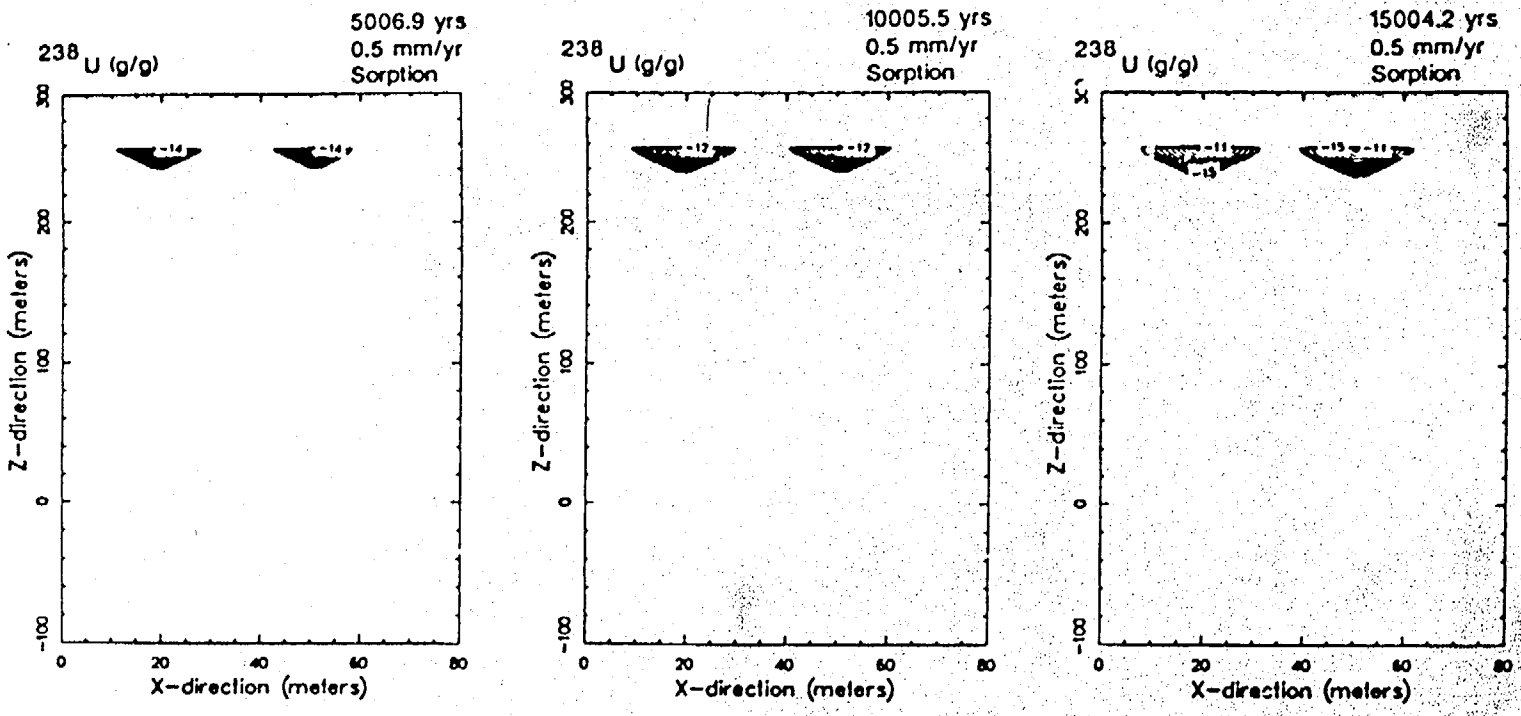

Figure 3. Sorbed concentrations during transport of ^{238}U through unsaturated Yucca Mountain tuff at normal flow rate. Adjacent lines differ in concentration by a factor of 10. u_z = 0.5 mm/yr. t = 5000, 10000, and 15000 yr. (Case 1)

0 0 3 8 6 0 5 4 2

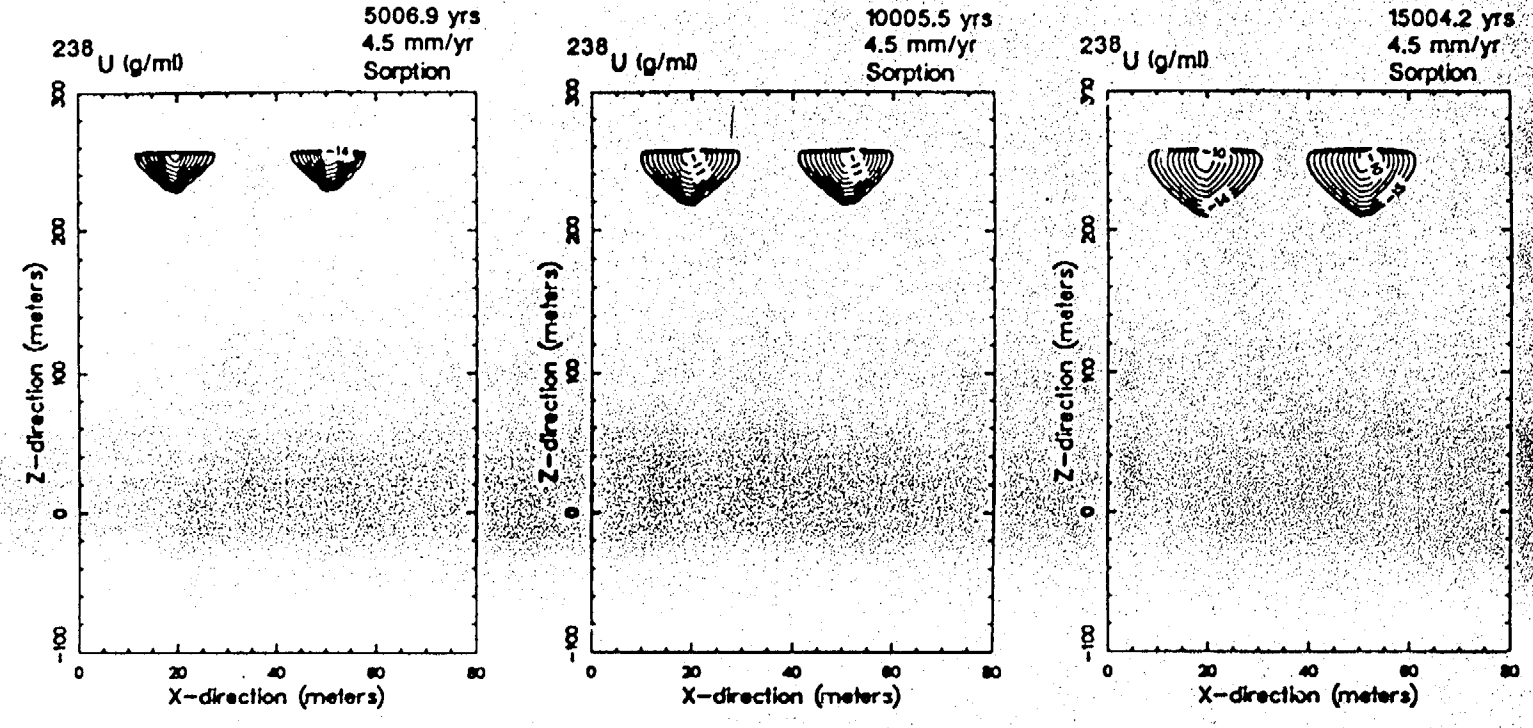

Figure 4. Liquid-phase concentrations during transport of ^{238}U through unsaturated Yucca Mountain tuff at high flow rate. Adjacent lines differ in concentration by a factor of 10. u_z = 4.5 mm/yr. t = 5000, 10000, and 15000 yr. (Case 2)

9038643

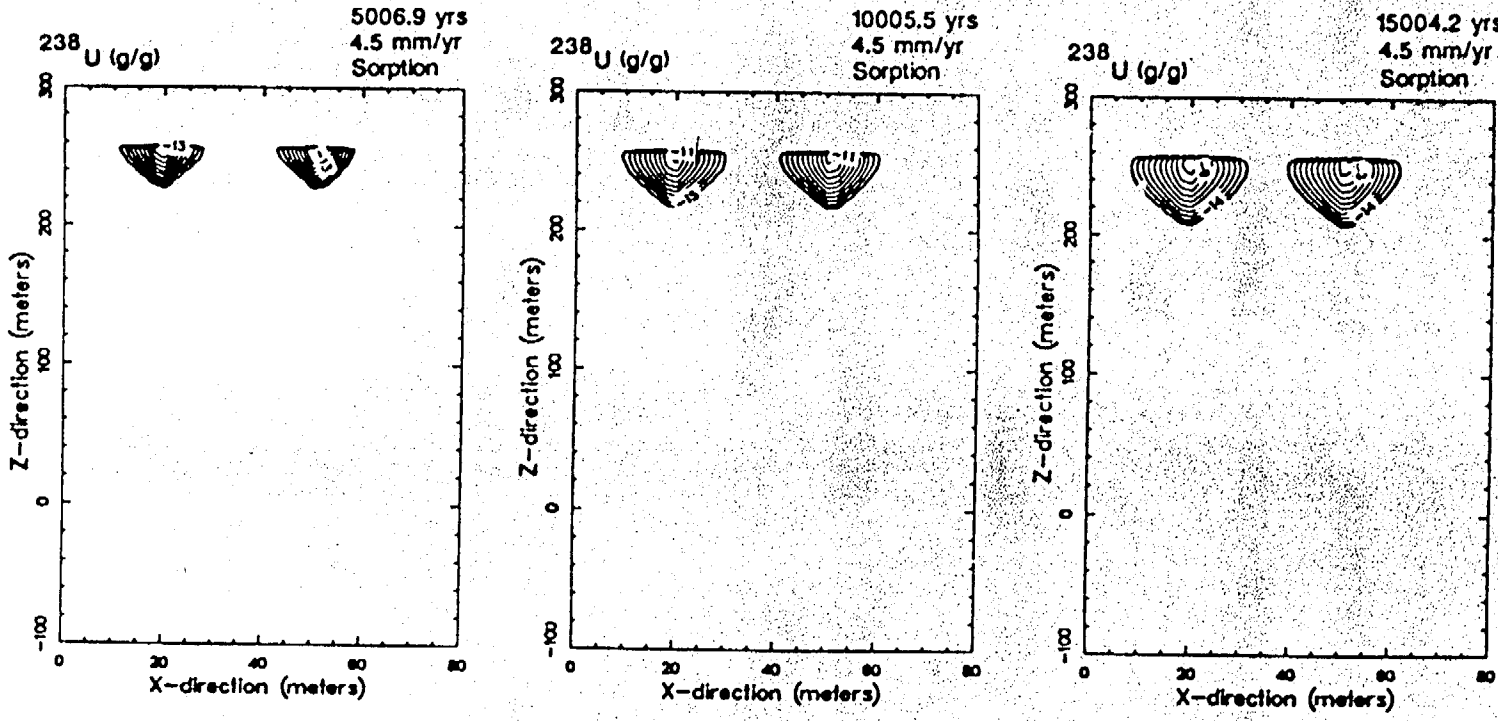

Figure 5. Sorbed concentrations during transport of ^{238}U through unsaturated Yucca Mountain tuff at high flow rate. Adjacent lines differ in concentration by a factor of 10. u_z = 4.5 mm/yr. t = 5000, 10000, and 15000 yr. (Case 2)

0 0 3 8 6 0 5 4 4

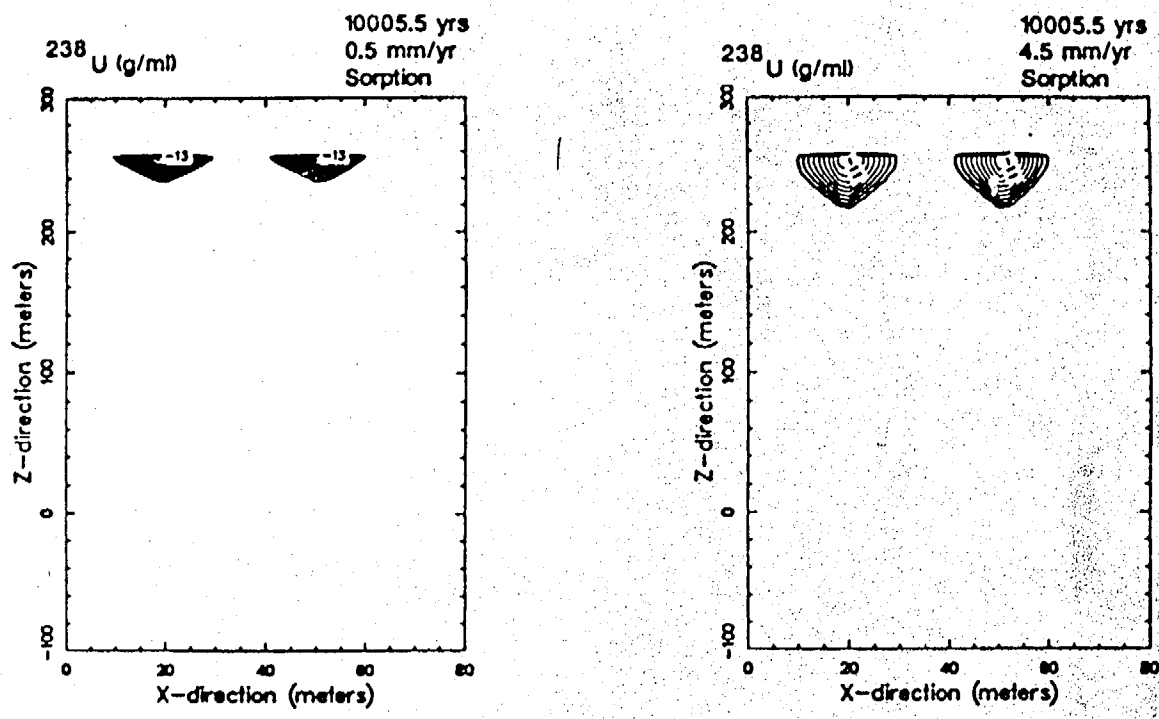

Figure 6. Comparison of liquid-phase concentrations of ^{238}U after transportfor 10000 yr at different flow rates (Cases 1 and 2). Adjacent lines differ in concentration by a factor of 10.

3 0 3 8 5 0 3 4 5

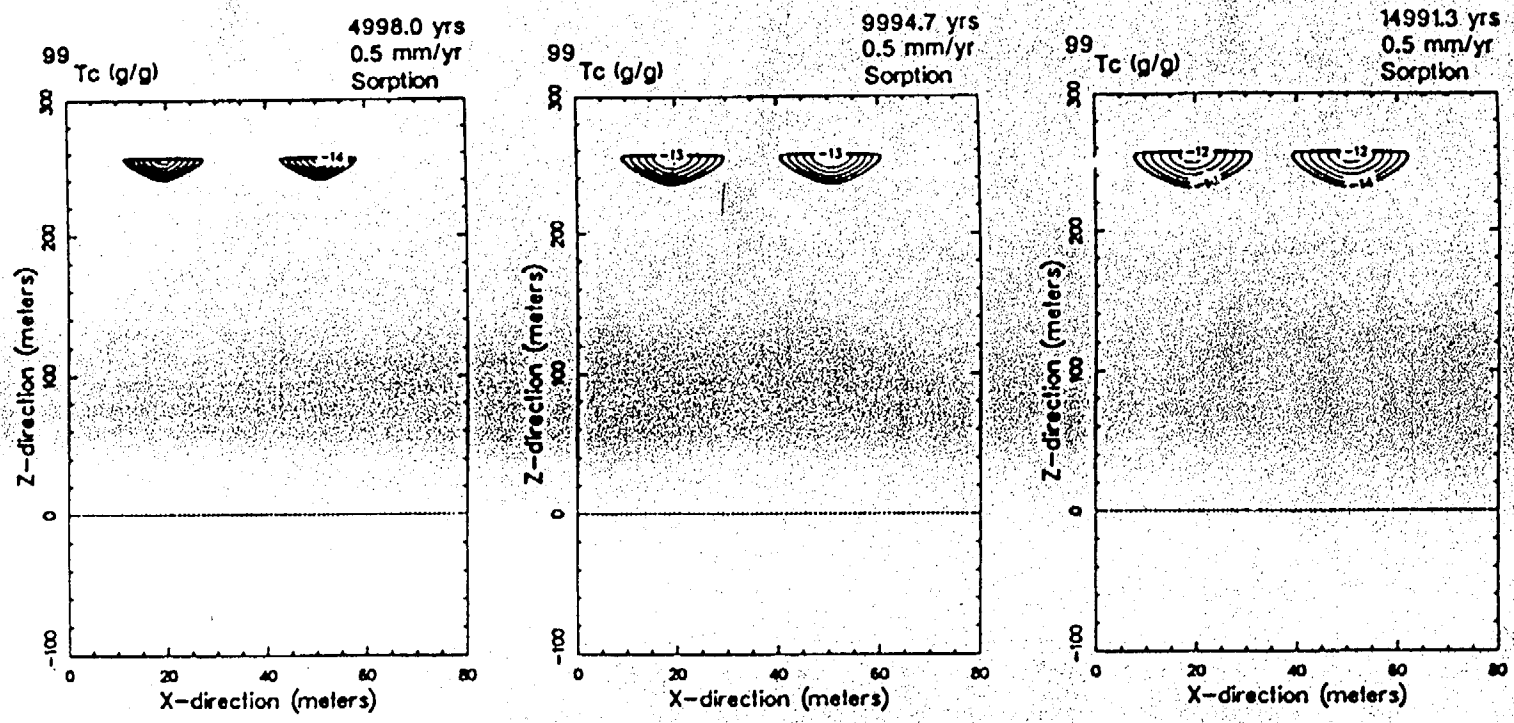

Figure 7. Liquid-phase concentrations during transport of ^{99}Tc with sorption through unsaturated Yucca Mountain tuff at normal flow rate. Adjacent lines differ in concentration by a factor of 10. u_z = 0.5 mm/yr. t = 5000, 10000, and 15000 yr. (Case 3)

0 0 3 8 6 0 5 4 6

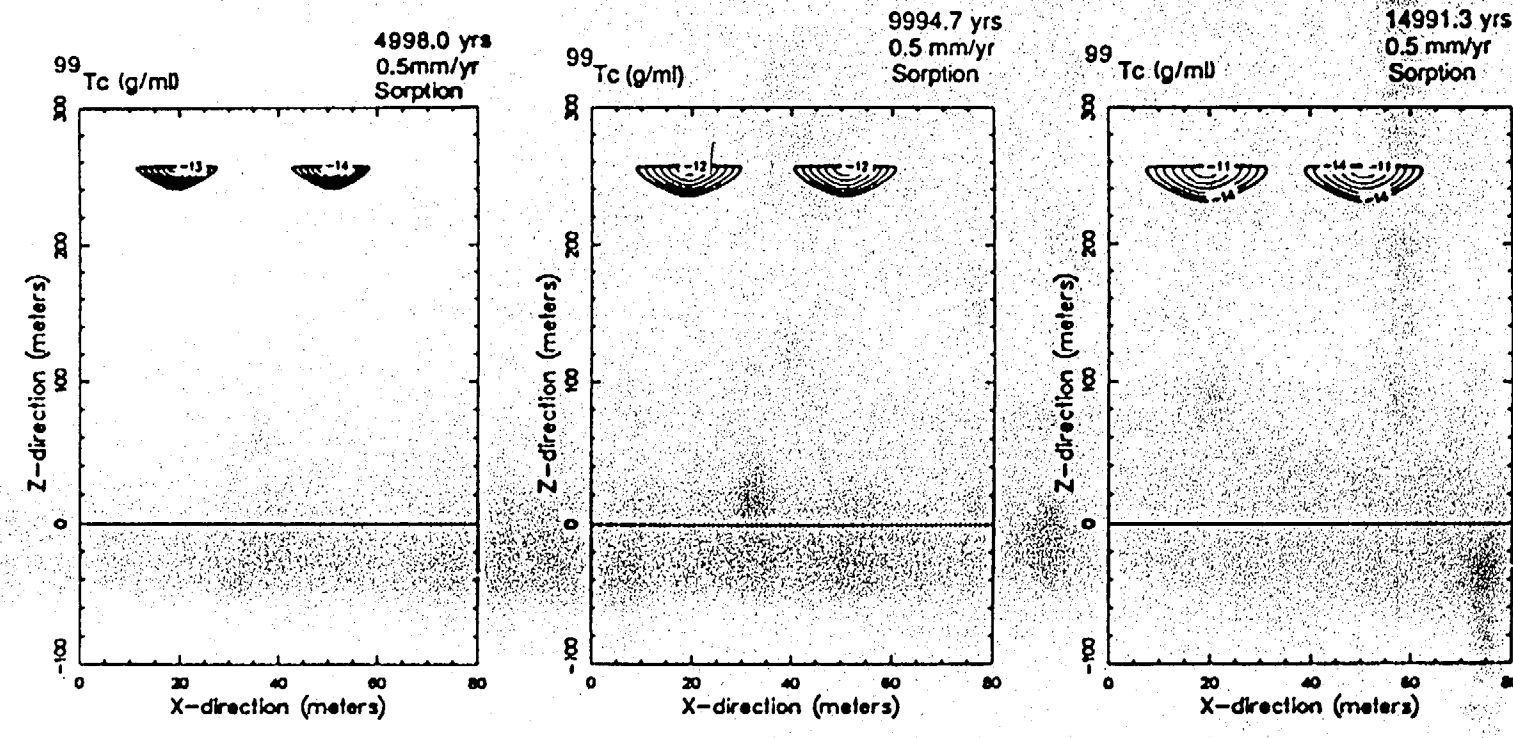

Figure 8. Sorbed concentrations during transport of ^{99}Tc with sorption through unsaturated Yucca Mountain tuff at normal flow rate. Adjacent lines differ in concentration by a factor of 10. u_z = 0.5 mm/yr. t = 5000, 10000, and 15000 yr. (Case 3)

3038547

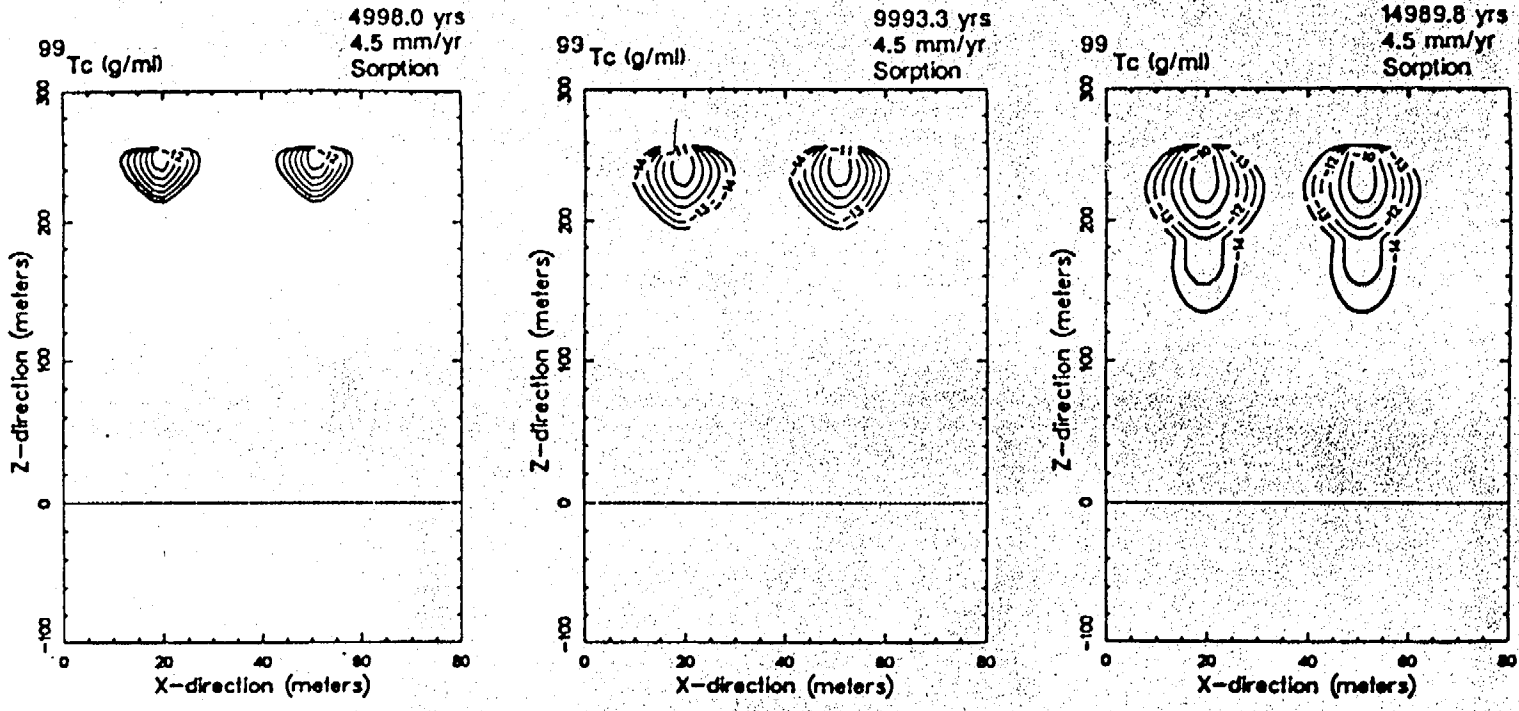

Figure 9. Liquid-phase concentrations during transport of ^{99}Tc with sorption through unsaturated Yucca Mountain tuff at high flow rate. Adjacent lines differ in concentration by a factor of 10. u_z = 4.5 mm/yr. t = 5000, 10000, and 15000 yr. (Case 4)

9038605348

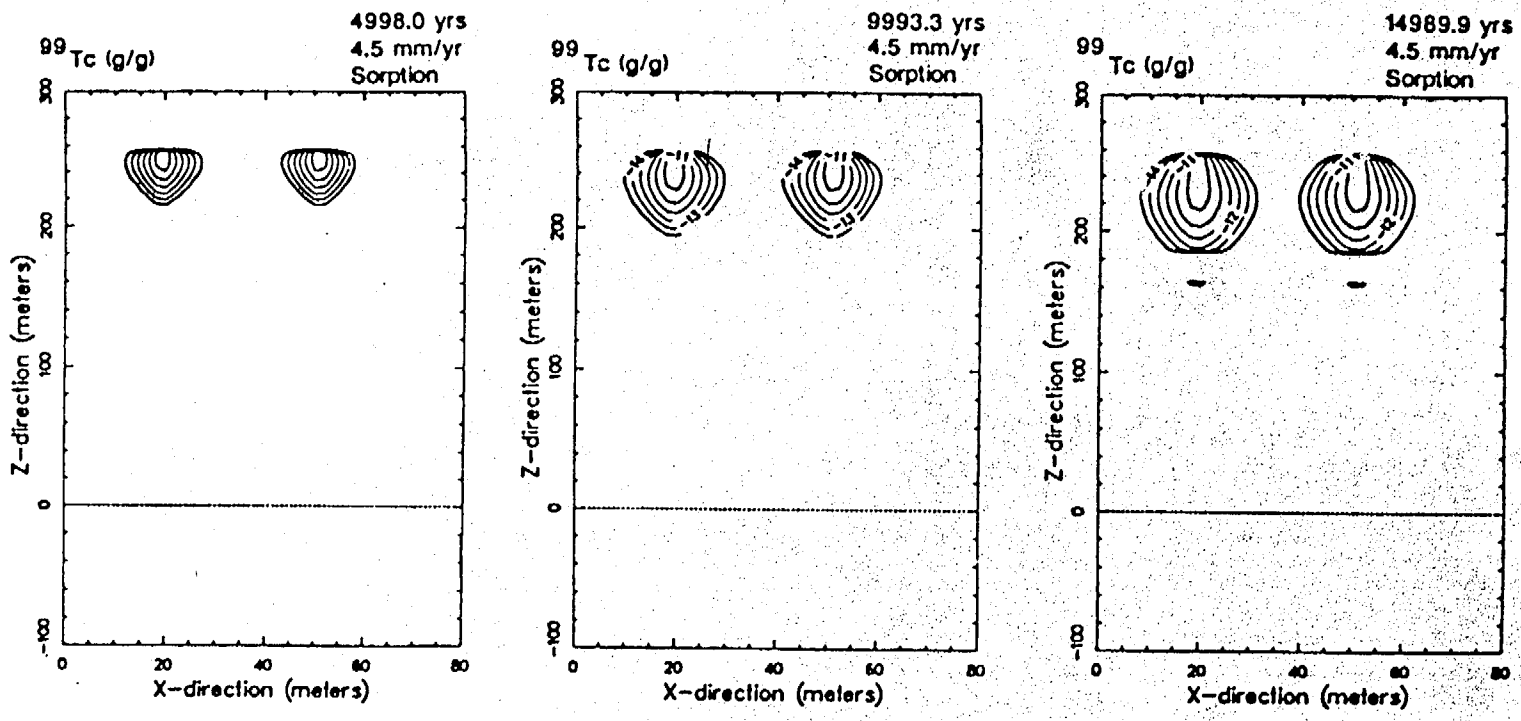

Figure 10. Sorbed concentrations during transport of ^{99}Tc with sorption through unsaturated Yucca Mountain tuff at high flow rate. Adjacent lines differ in concentration by a factor of 10. u_z = 4.5 mm/yr. t = 5000, 10000, and 15000 yr. (Case 4)

9 0 3 8 6 0 5 4 9

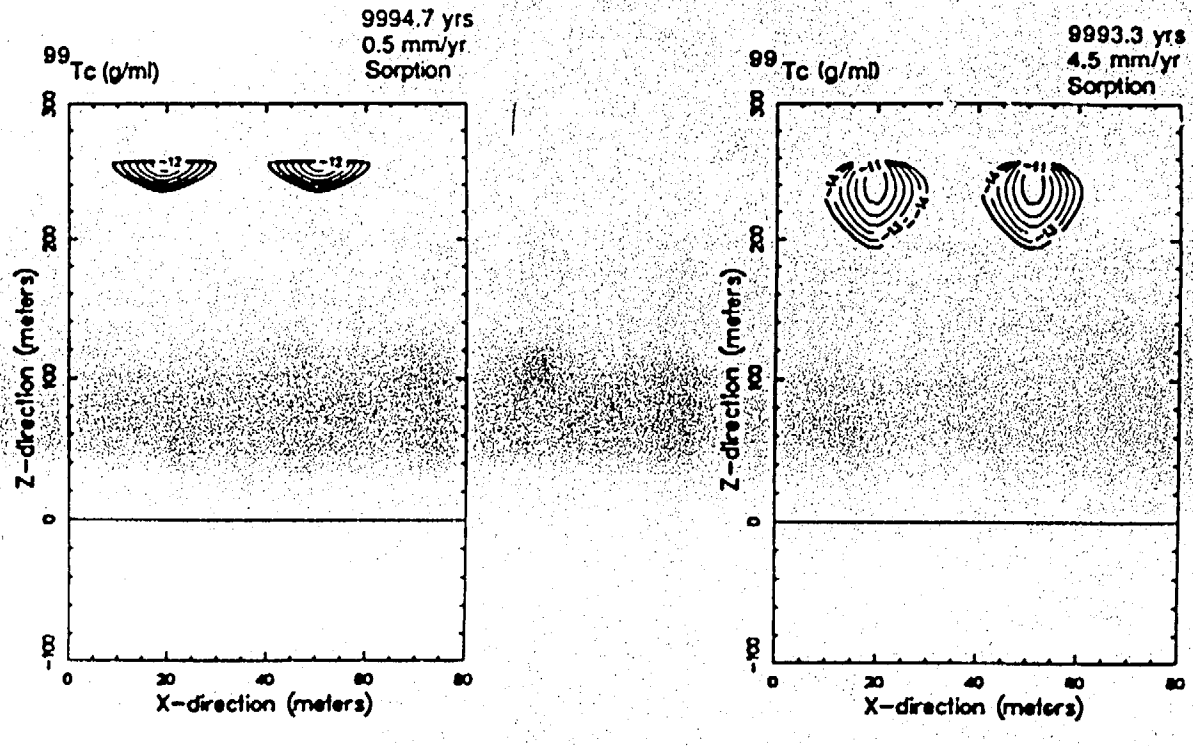

Figure 11. Comparison of liquid-phase concentrations of ^{99}Tc after transport with sorption for 10000 yr at different flow rates (Cases 3 and 4). Adjacent lines differ in concentration by a factor of 10.

0 5 5 0 3 8 6

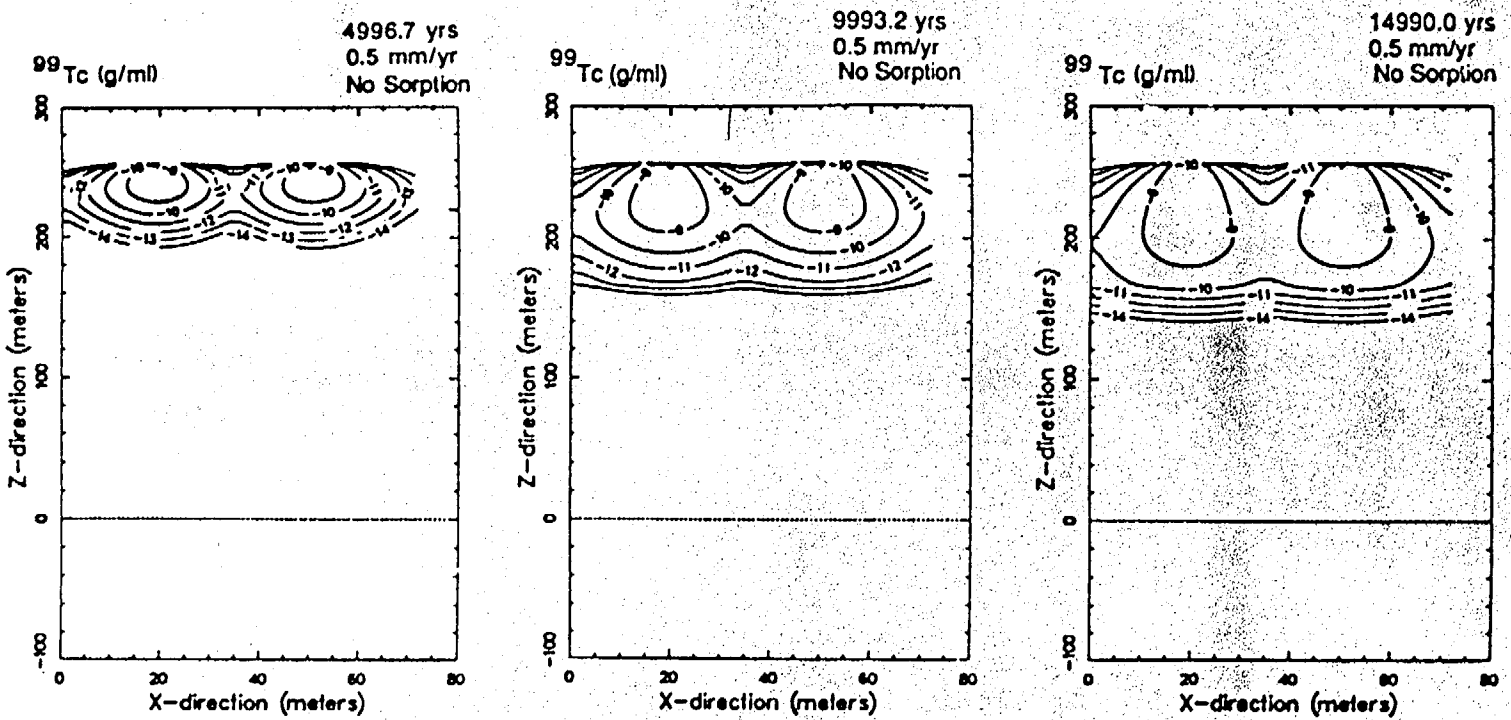

Figure 12. Liquid-phase concentrations during transport of ^{99}Tc without sorption through unsaturated Yucca Mountain tuff at normal flow rate. Adjacent lines differ in concentration by a factor of 10. u_z = 0.5 mm/yr. t = 5000, 10000, and 15000 yr. (Case 5)

0 0 3 8 5 0 5 5 1

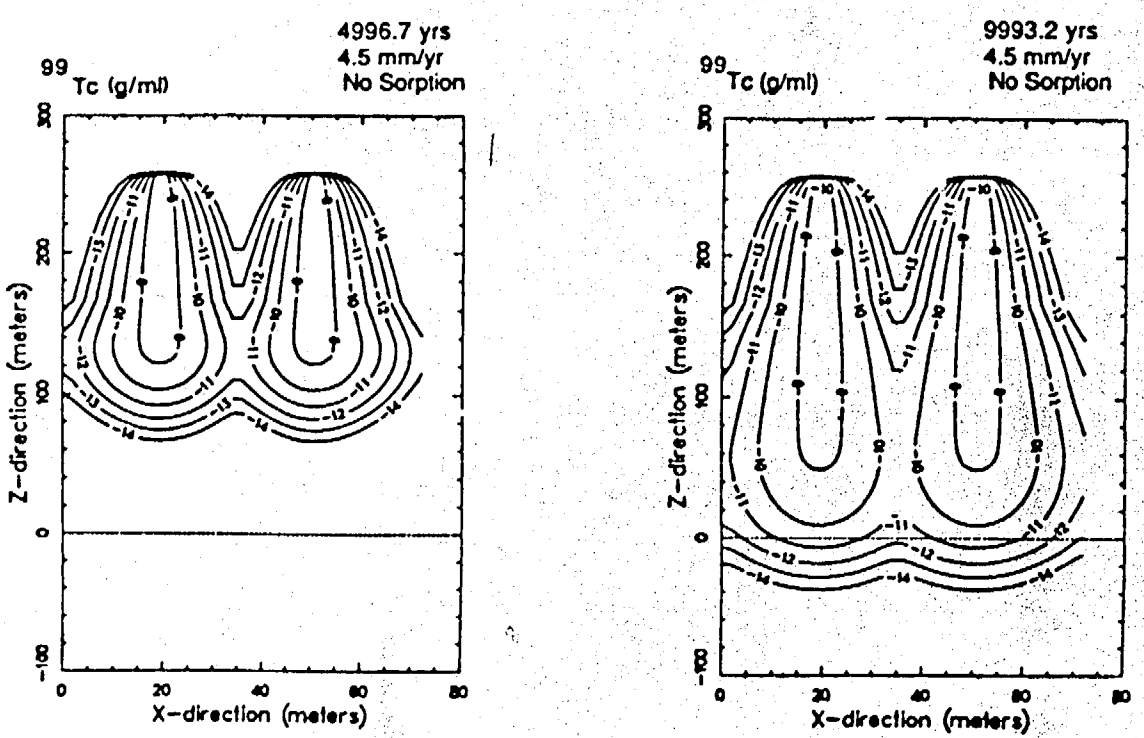

Figure 13. Liquid-phase concentrations during transport of ^{99}Tc without sorption through unsaturated Yucca Mountain tuff at high flow rate. Adjacent lines differ in concentration by a factor of 10. u_z = 4.5 mm/yr. t = 5000 and 10000 yr. (Case 6)

7 0 3 3 6 0 5 5 2

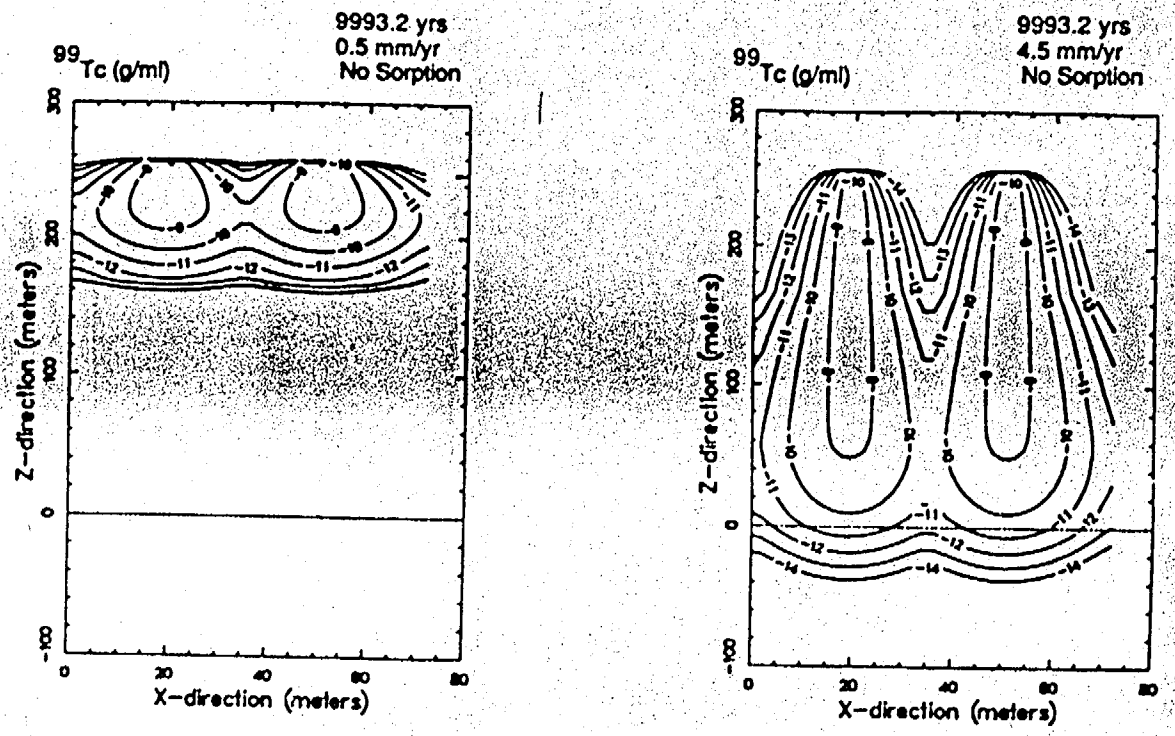

Figure 14. Comparison of liquid-phase concentrations of ^{99}Tc after transport without sorption for 10000 yr at different flow rates (Cases 5 and 6). Adjacent lines differ in concentration by a factor of 10.

9 0 3 8 5 0 5 5 3

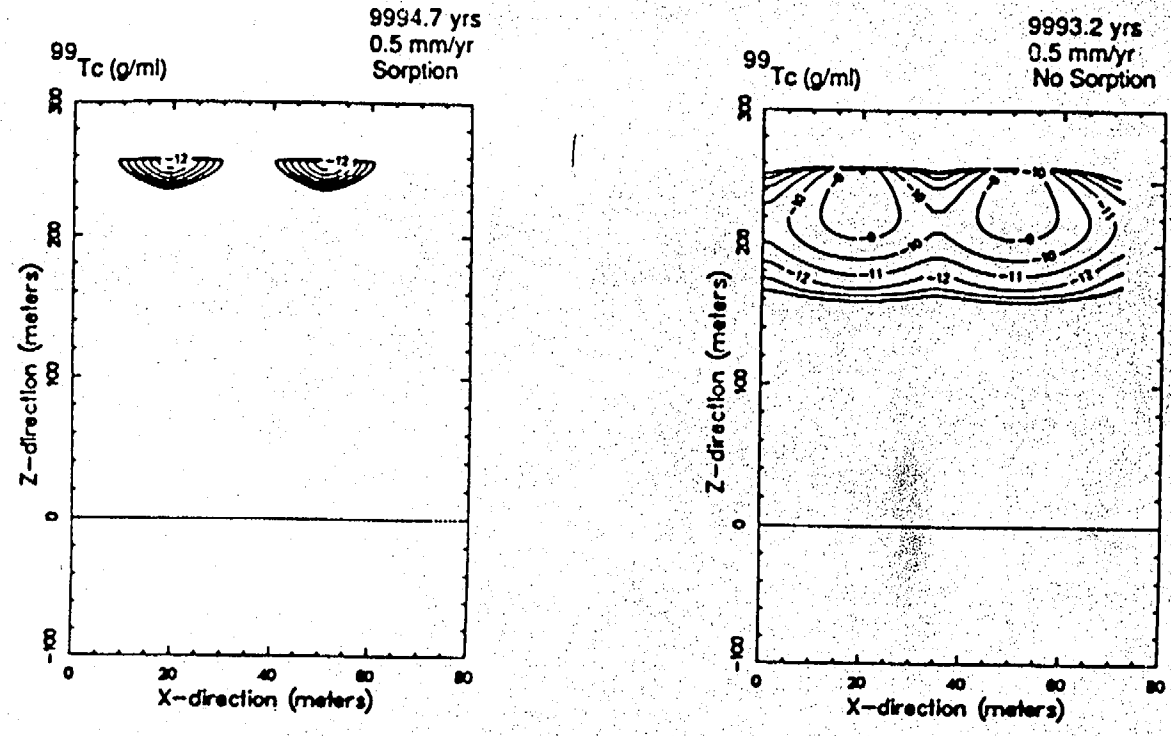

Figure 15. Effect of sorption on liquid-phase concentration of ^{99}Tc after transport through Yucca Mountain tuff at normal flow rate for 10000 yr. Adjacent lines differ in concentration by a factor of 10. u_z = 0.5 mm/yr. (Cases 3 and 5)

203865 0554

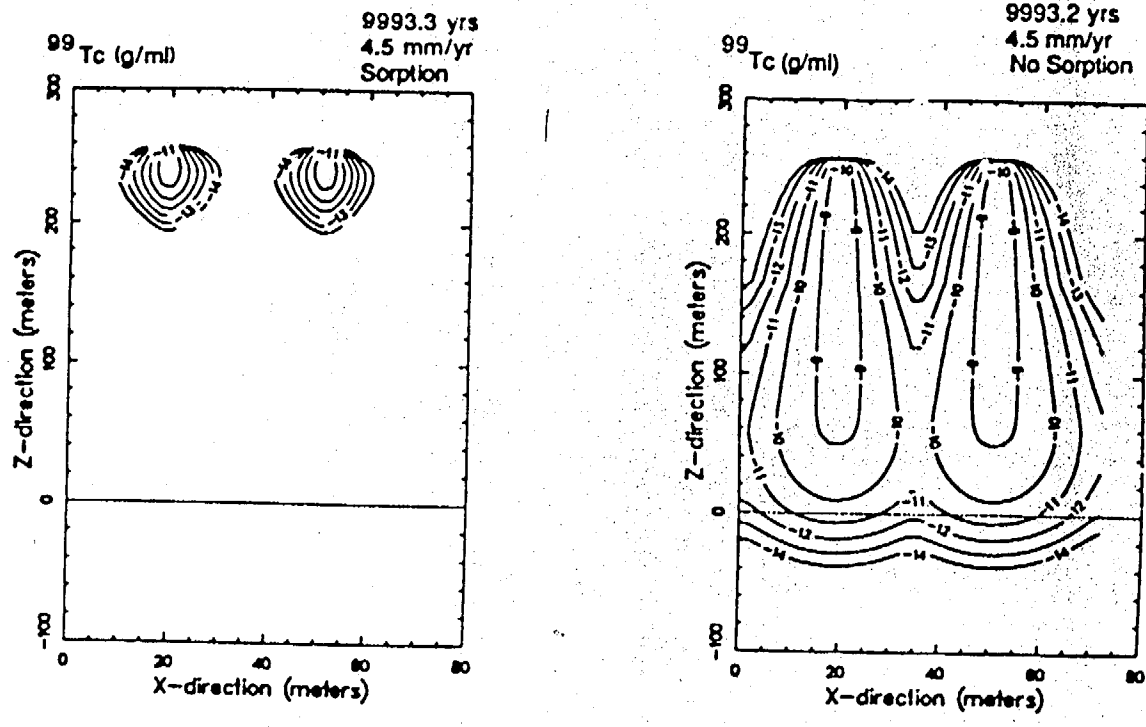

Figure 16. Effect of sorption on liquid-phase concentration of ^{99}Tc after transport through Yucca Mountain tuff at normal flow rate for 10000 yr. Adjacent lines differ in concentration by a factor of 10. u_z = 0.5 mm/yr. (Cases 4 and 6)

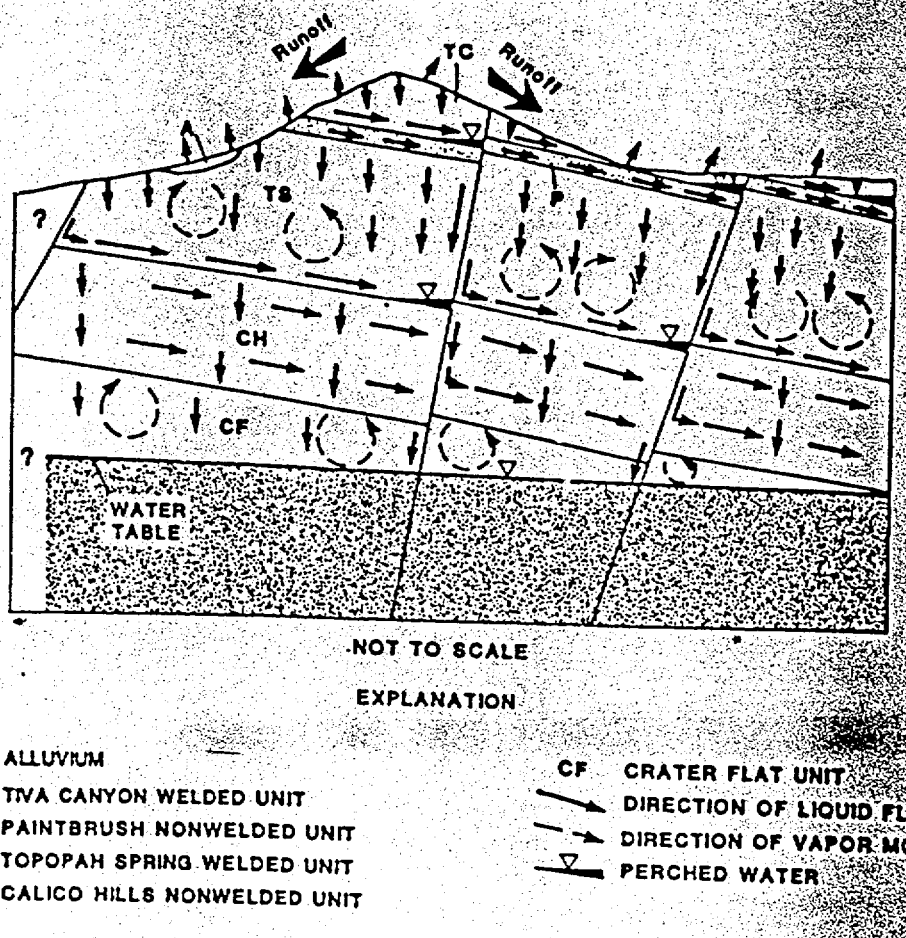

Figure 17. Hypothesized model of the flow regime through the hydrogeologic units at Yucca Mountain (Motazer and Wilson 1984, Fig. 14; reprinted with permission)